Searching for Galactic Axions: QUAX Experiment

QUest for AXions

Giovanni Carugno

on behalf of the QUAX Collaboration

Outlines:

- Cosmological Axion Detection Schemes Principles
- Haloscopes Components
- Quantum Linear Amplifier JPA vs TWPA
- Single Photon Microwave Detector
- Perspectives & Conclusions

QUAX – QUaerere AXion

- Detection of **cosmological axions** through their **coupling to electrons or photons**
- **Electron coupling: Due to the motion of the solar system** in the galaxy, the axion DM cloud acts as an **effective RF magnetic field** on electron spin exciting magnetic transitions in a magnetized sample and **producing rf photons**

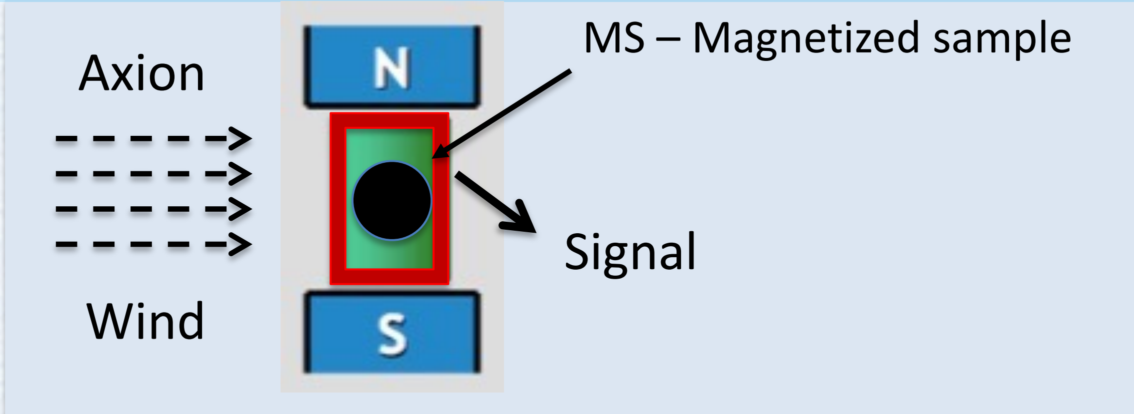

QUAX-ae

- **Photon coupling: DM axion** are converted into **rf photons** inside a **resonant cavity** immersed in a **strong magnetic field**

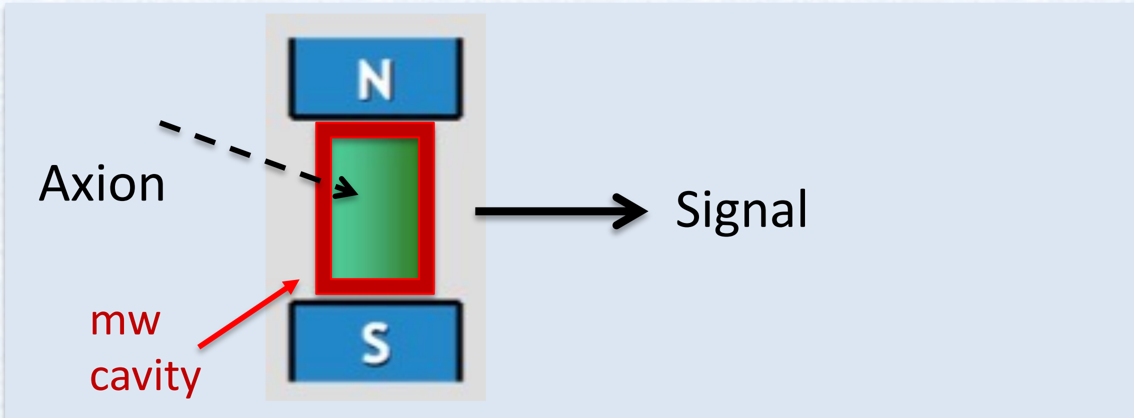

QUAX-aγ

Axion interactions

All couplings are extremely weak **(Invisible Axion models)**!

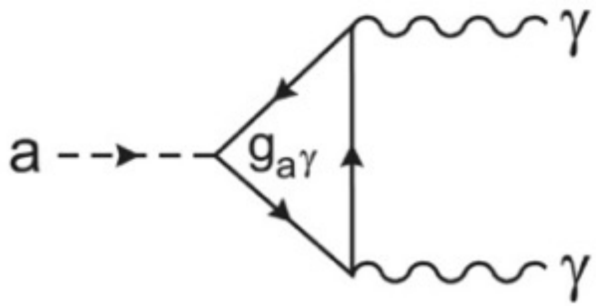

Axion photon photon (Inverse Primakoff effect)

$$\mathcal{L}_{a\gamma\gamma} = -\left(\frac{\alpha}{\pi}\frac{g_\gamma}{f_a}\right) a\vec{E}\cdot\vec{B} = -g_{a\gamma\gamma} a\vec{E}\cdot\vec{B}$$

$$g_{a\gamma\gamma} = g_\gamma \frac{\alpha}{\pi}\frac{m_a}{m_\pi f_\pi}$$

g_γ = 0.36 (DFSZ)

g_γ = - 0.97 (KSVZ)

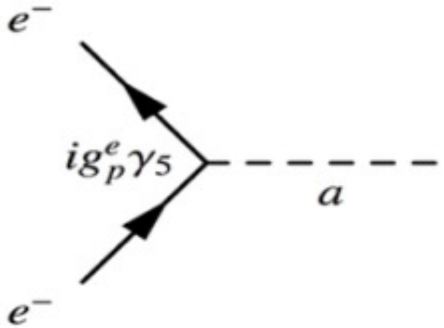

Axion electron electron

$$L_{aee} = -g_e \bar{e} i\gamma_5 e a$$

$$\frac{g_p \hbar}{2m}\boldsymbol{\sigma}\cdot\boldsymbol{\nabla} a$$

Non relativistic electron

$$g_e \approx \frac{m_a m_e}{m_\pi f_\pi} = 4.07\times 10^{-11} m_a$$ **(DFSZ)**

g_e ~ 0 (Strongly suppressed) (KSVZ)

Detection scheme: electron coupling

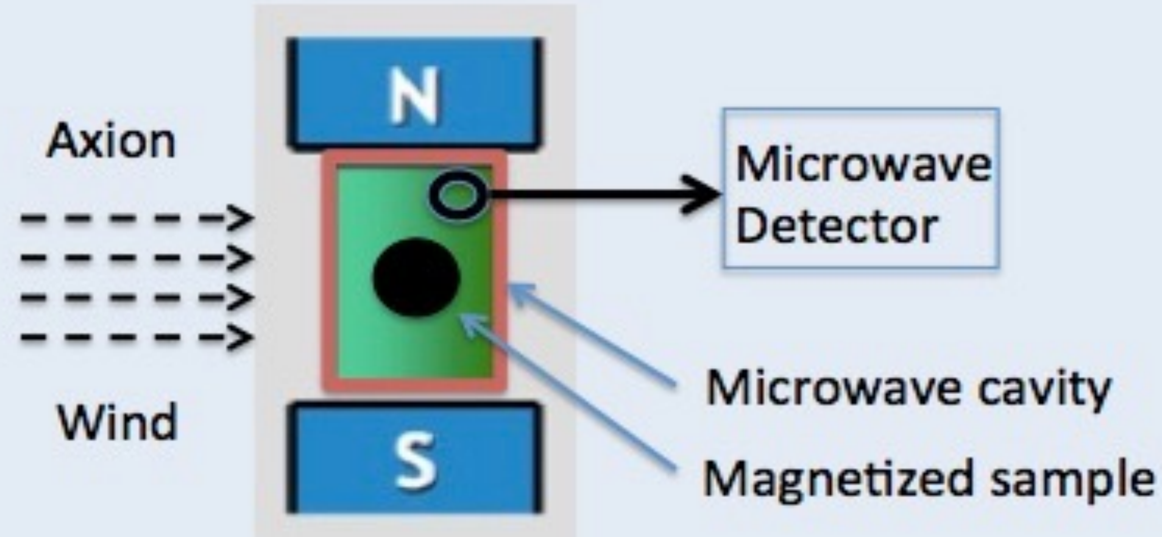

Axion induced magnetization

$$M_a(t) = \gamma \mu_B B_a n_S \tau_{\min} \cos(\omega_a t),$$

Power emitted from magnetized sample

$$P_{\text{out}} = \frac{P_{\text{in}}}{2} = 8 \times 10^{-26} \left(\frac{m_a}{2 \cdot 10^{-4}\,\text{eV}}\right)^3 \left(\frac{V_s}{1\ \text{liter}}\right) \left(\frac{n_S}{10^{28}/\text{m}^3}\right) \left(\frac{\tau_{\min}}{10^{-6}\,\text{s}}\right) \text{W},$$

Final experiment to be performed with a microwave quantum counter

$$R_a = \frac{P_{\text{out}}}{\hbar \omega_a} = 2.6 \times 10^{-3} \left(\frac{m_a}{2 \cdot 10^{-4}\,\text{eV}}\right)^2 \left(\frac{V_s}{1\ \text{liter}}\right) \left(\frac{n_S}{10^{28}/\text{m}^3}\right) \left(\frac{\tau_{\min}}{10^{-6}\,\text{s}}\right) \text{Hz.} \tag{17}$$

Key elements:

- **High Q microwave cavity** operating in a static magnetic field (about 1 T)
- **Magnetic material** with long relaxation time (~ 1 μs) and high spin density
- **Magnetic field** with high stability and homogeneity (at ppm level)
- Microwave **quantum counter**
- Integration and operation at **ultra cryogenic temperature (about 0.1 K)**

Axion driving of magnetization

The axion wind mimics the transverse rf magnetic field inducing a **time dependent magnetization of the uniform or Kittel mode** of the magnetized sample

$$M_a(t) = \gamma \mu_B B_a n_S \tau_{\min} \cos(\omega_a t),$$

at resonance

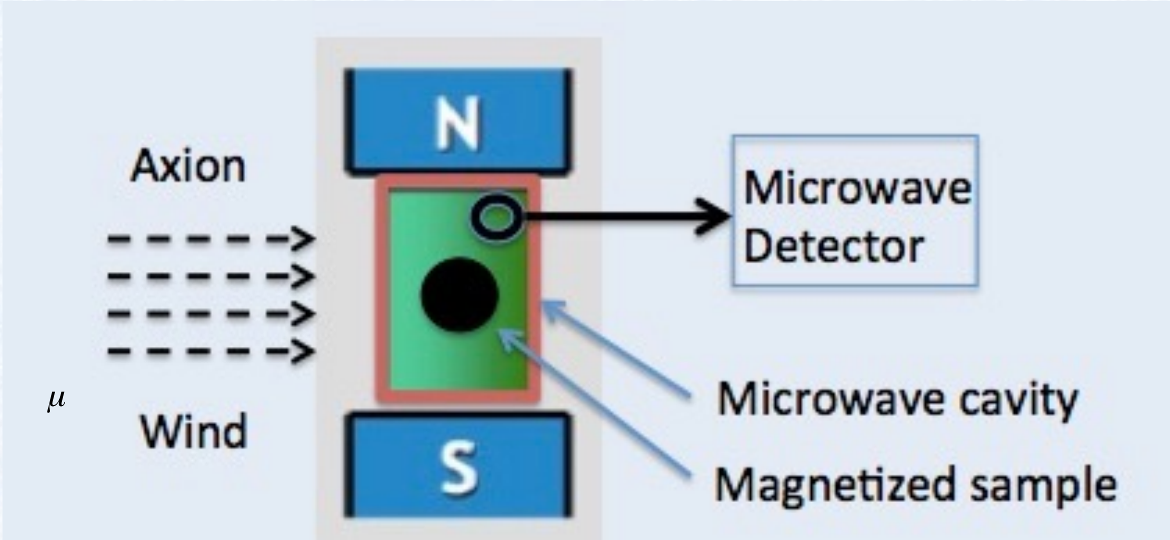

τ_{min} is the shortest coherence time among:

- **axion wind** coherence $\tau_{\nabla a}$
- magnetic material **relaxation time τ_2**
- **radiation damping τ_r**

n_s – material spin density

μ_B – Bohr magneton

A **volume V_s of magnetized material** will absorb energy from $\mathbf{B}_a$ at a rate

$$P_{\text{in}} = \mu_0 \mathbf{H} \cdot \frac{d\mathbf{M}}{dt} = B_a \frac{dM_a}{dt} V_s = \gamma \mu_B n_S \omega_a B_a^2 \tau_{\min} V_s$$

this power will excite magnetization/cavity modes and could be possibly detected

The axion effective magnetic field

- R. Barbieri et al., *Searching for galactic axions through magnetized media: The QUAX proposal* [Phys. Dark Univ. **15,** 135 - 141 (2017)]

The effective magnetic field associated with the axion wind

$$B_a = \frac{g_p}{2e}\left(\frac{n_a h}{m_a c}\right)^{1/2} m_a \mathrm{v}_E$$

n_a – axion density ~ 0.4 Gev/cm^3
v_E – Earth velocity ~220 km/s
axion velocity dispersion ~270 km/s

Using from standard model of Galactic Halo:

$$B_a = 2.0 \cdot 10^{-22} \left(\frac{m_a}{200\,\mu\mathrm{eV}}\right) \mathrm{T},$$

$$\frac{\omega_a}{2\pi} = 48 \left(\frac{m_a}{200\,\mu\mathrm{eV}}\right) \mathrm{GHz},$$

$$\tau_{\nabla a} \simeq 0.68\,\tau_a = 17 \left(\frac{200\,\mu\mathrm{eV}}{m_a}\right)\left(\frac{Q_a}{1.9 \times 10^6}\right) \mu\mathrm{s};$$

Coherence time

$$\lambda_{\nabla a} \simeq 0.74\,\lambda_a = 5.1 \left(\frac{200\,\mu\mathrm{eV}}{m_a}\right) \mathrm{m},$$

Correlation length

Anticipated signal strength

Expected signal as a function of relevant experimental parameters

Working @ m_a = 200 meV-> 48 GHz

Larmor frequency tuning by magnetizing field
B_0 = 1.7 T => 48 GHz

$$P_{\text{out}} = \frac{P_{\text{in}}}{2} = \mathbf{3.8 \times 10^{-26}} \left(\frac{m_a}{200\,\mu\text{eV}}\right)^3 \left(\frac{V_s}{100\ \text{cm}^3}\right) \left(\frac{n_S}{2 \cdot 10^{28}/\text{m}^3}\right) \left(\frac{\tau_{\text{min}}}{2\,\mu\text{s}}\right) \text{W}$$

Such a low power level is out of reach of linear amplifiers → **Single photon microwave detection**

See discussion in *S.K. Lamoreaux et al., Phys. Rev. D 88 (2013) 035020.*

The corresponding **signal photon rate**

$$R_a = \frac{P_{\text{out}}}{\hbar\omega_a} = \mathbf{1.2 \times 10^{-3}}\ \text{Hz}$$

this rate establishes the required dark count rate of the photon counter

Detection scheme: photon coupling

The same set-up can be operated as a Sikivie's haloscope to study Axion-Photon coupling

$$P_{\mathrm{a}} = 1.85 \times 10^{-25}\,\mathrm{W} \left(\frac{V}{0.0361}\right) \left(\frac{B}{2\,\mathrm{T}}\right)^2 \left(\frac{g_\gamma}{-0.97}\right)^2 \times \left(\frac{C}{0.589}\right) \left(\frac{\rho_a}{0.45\,\mathrm{GeV\,cm^{-3}}}\right) \left(\frac{\nu_c}{9.067\,\mathrm{GHz}}\right) \left(\frac{Q_L}{201000}\right)$$

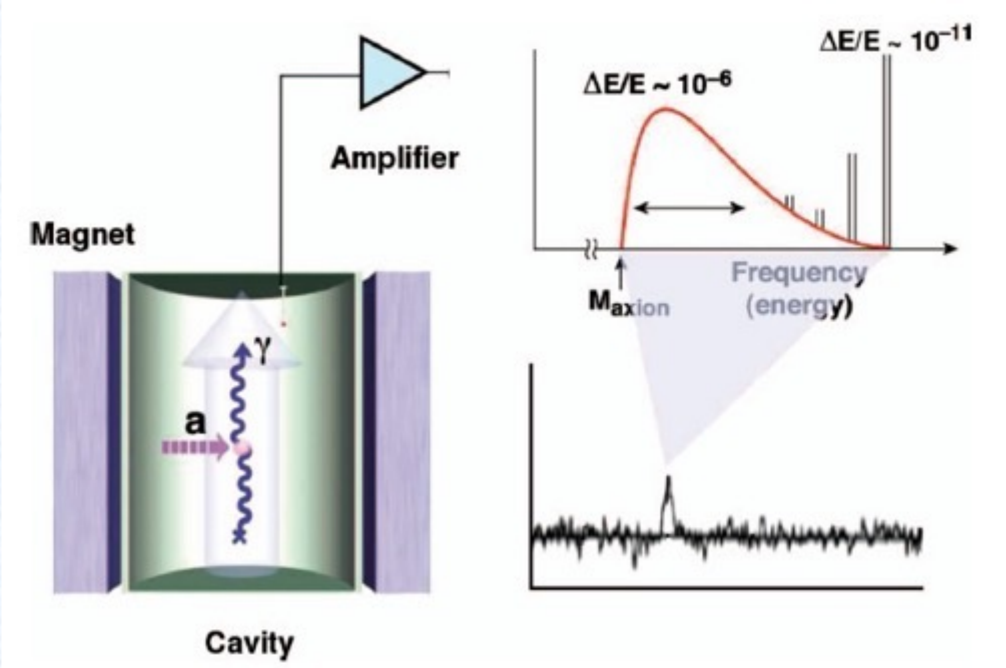

$$-\frac{\alpha}{8\pi}\frac{C_{a\gamma}}{f_a}\, a\, F_{\mu\nu}\tilde{F}^{\mu\nu}$$

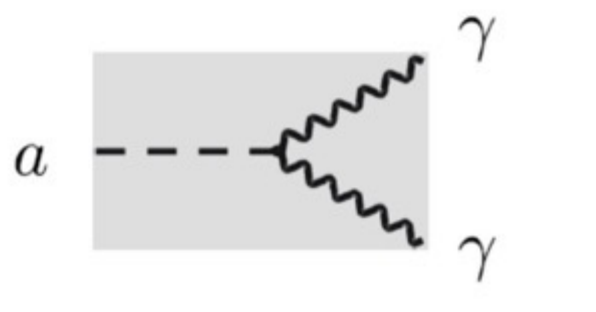

Key elements:

- **Avoid** the use of the **magnetic material**
- Resonant cavity mode High Q under strong B field
- Operate the magnet at **highest magnetic field amplitude**
- **Detection chain is the same**

Dilution Units (2 WET + 2 DRY)

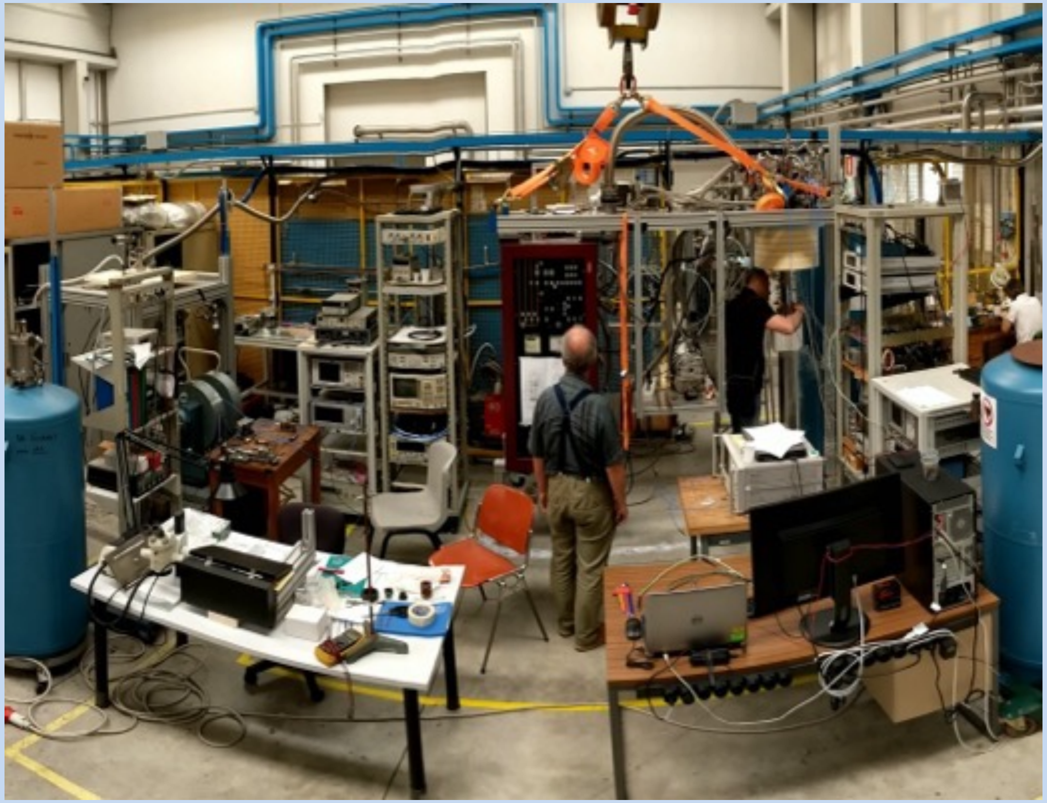

Low Power Dilution Unit

100 microWatt @ 100 milliKelvin

Working for axion-electron JPA

8 Kg of Copper + Electronic @ 100 mK

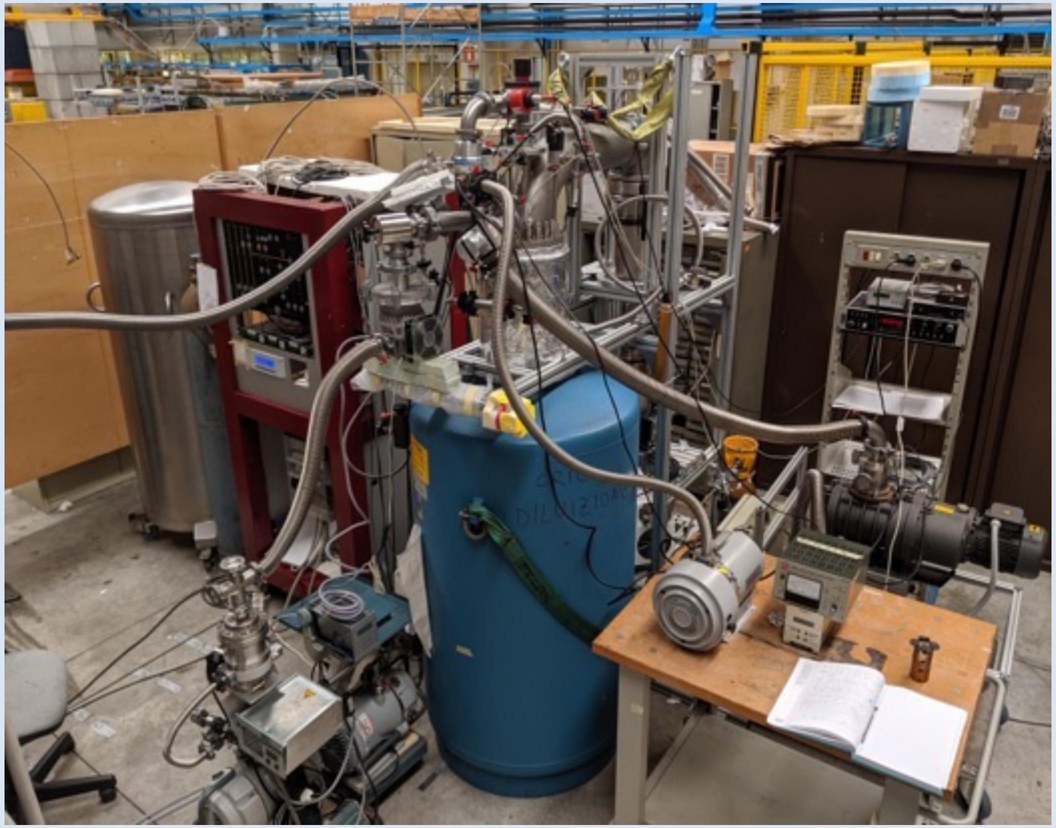

Large Power Dilution Unit

1 milliWatt @ 100 milliKelvin

Working for axion-gamma TWPA

Set up operational temperature 50 mK

Single Microwave Photon Detector in Italy

Paris run was successful the device will be mounted @ LNL

Electronics layout

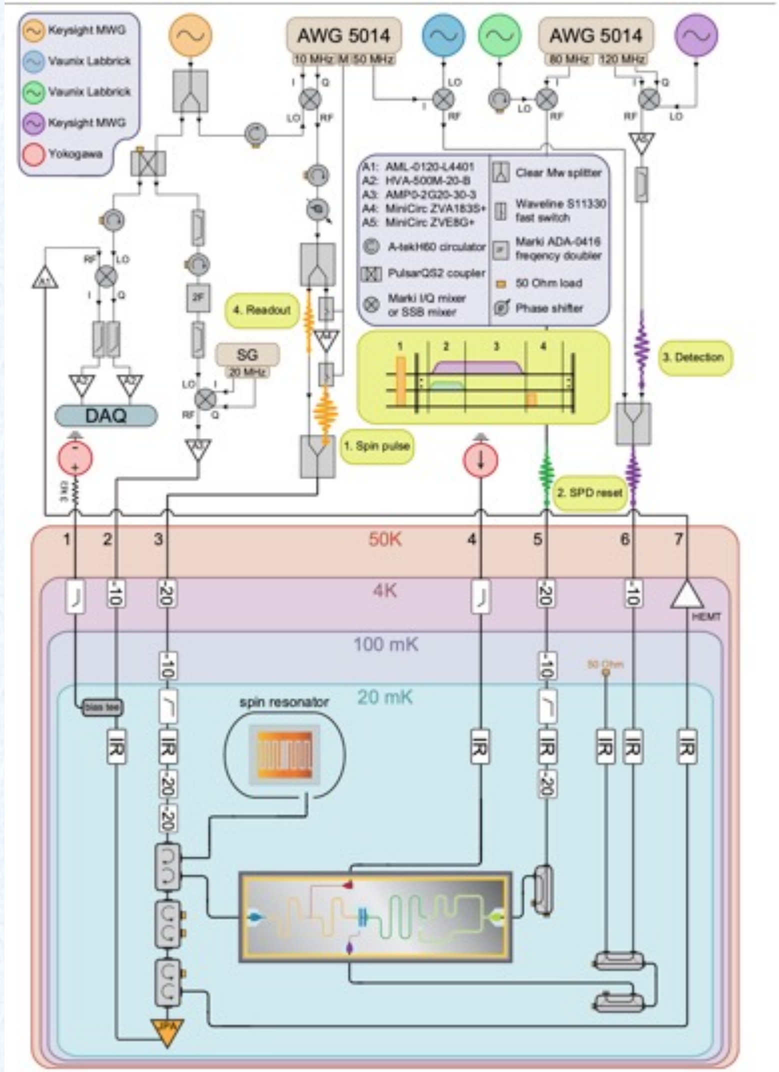

Leiden Cryogenics
commissioning in October 2022

Static magnetic field Homogeneity @ 2 T Magnet

- a 2 T magnet is now operating in the low power dilution system
- This magnet provides the high homogeneity necessary for the **axion electron search**

20 ppm field homogeneity

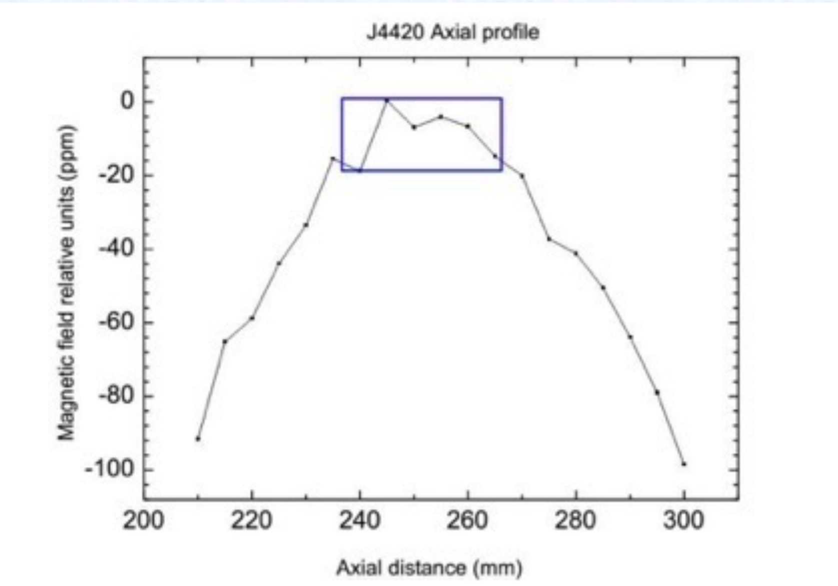

Static Magnetic field: 8 Tesla Magnet

Strong field for axion photon search

Superconducting coil NbTi

8 Tesla at 100 A @ 4 Kelvin

Length 48 cm , Bore 15 cm

14 Tesla Magnet Soon

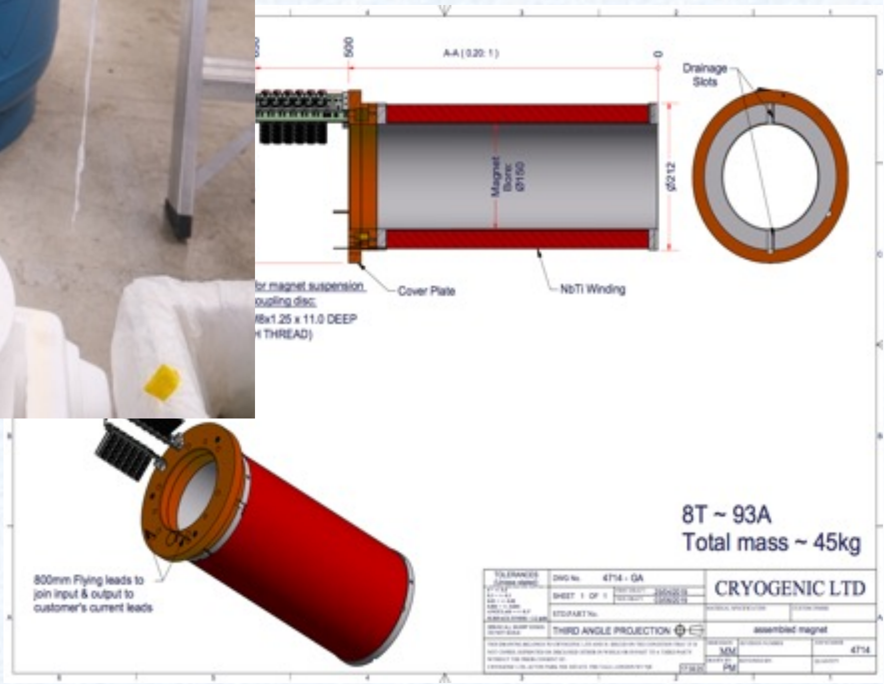

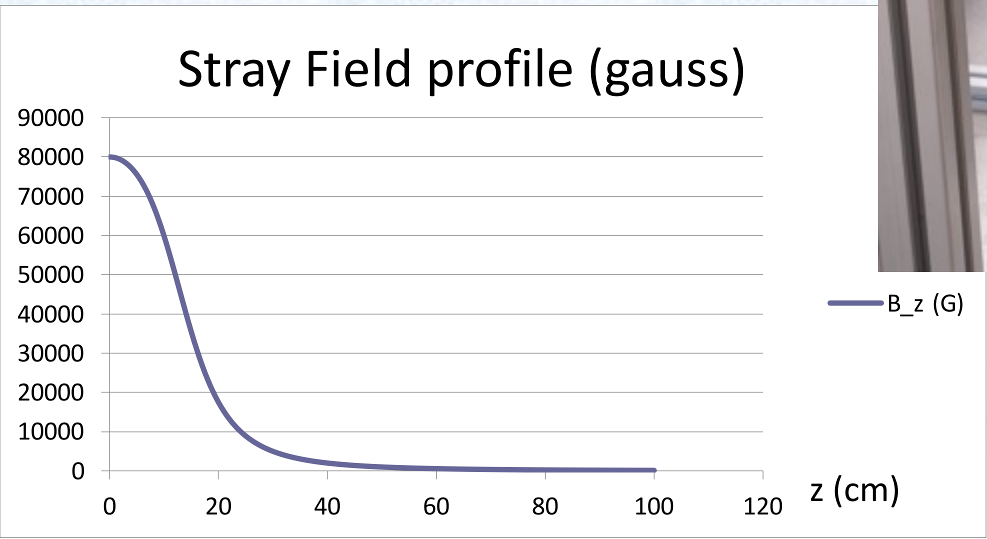

High Q RF Dielectric Cavity

First realization of a **dielectric cavity** made by two concentric sapphire cylinders to operate in a strong magnetic field

Exceptional Q value ~ 10 Million in an 8 T field

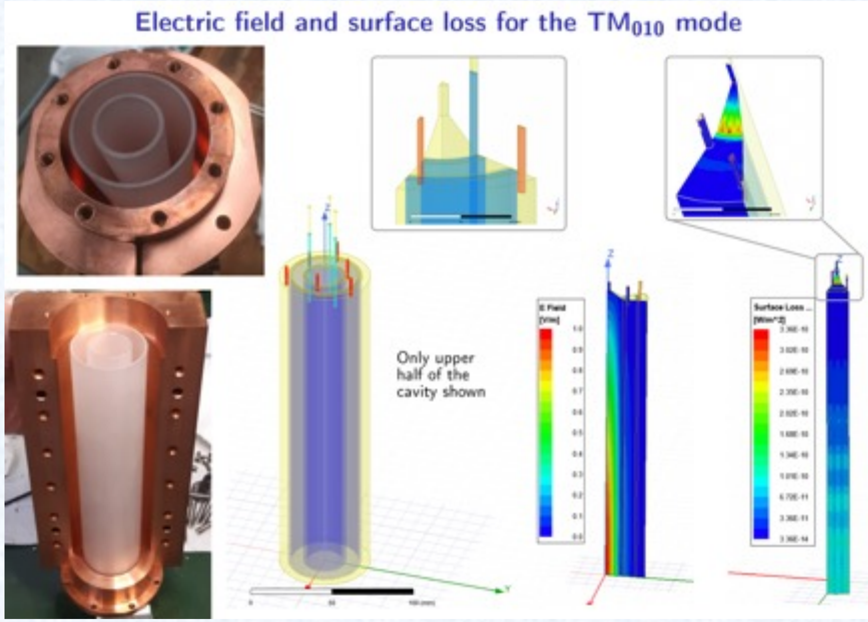

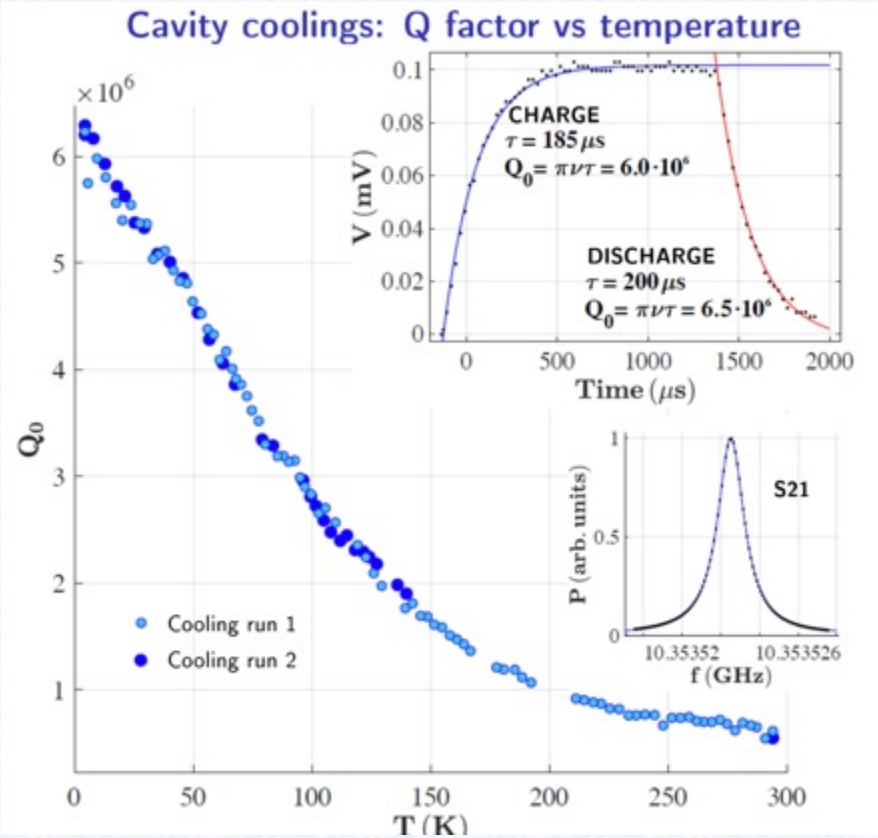

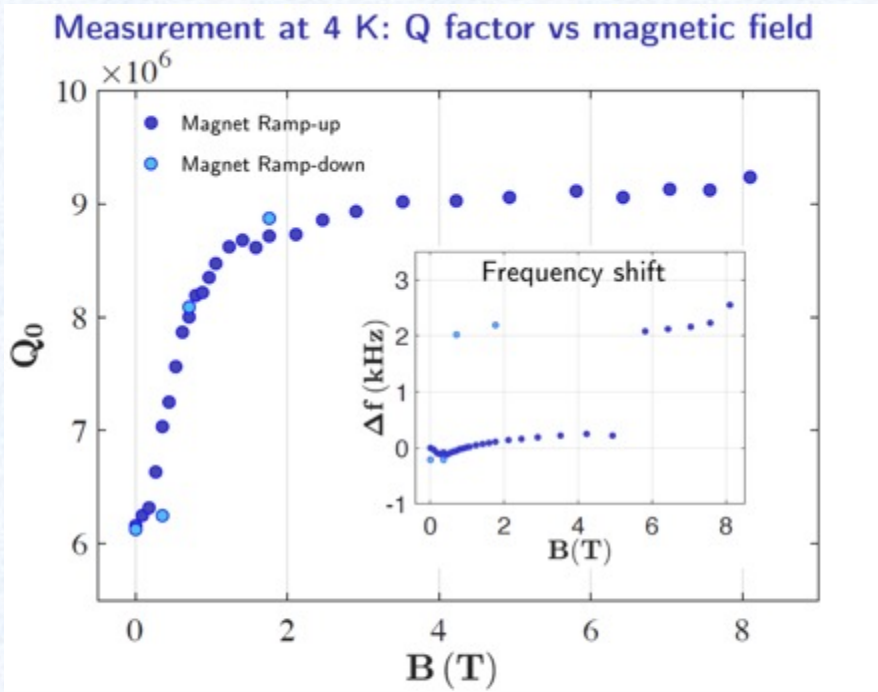

Cavity developments

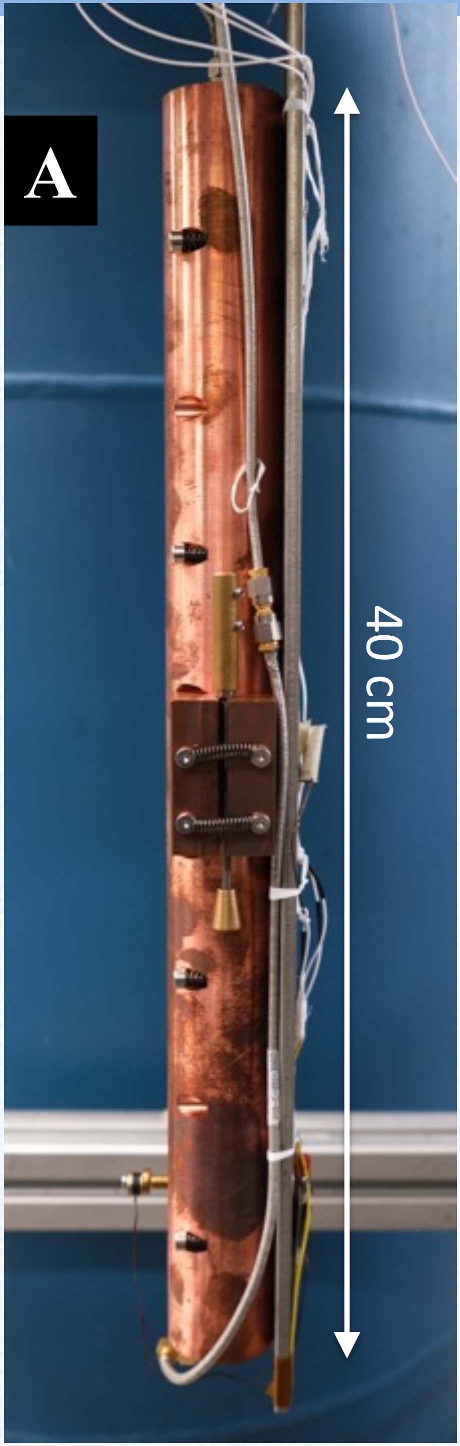

Three different novel cavity designs are being studied to maximize **$C^2 V^2 Q$**:

A. Empty "double-shell" cylindrical cavity with simple tuning

B. High volume, high C factor single-shell dielectrical cavity

C. High volume, high C factor empty "polygonal" cavity

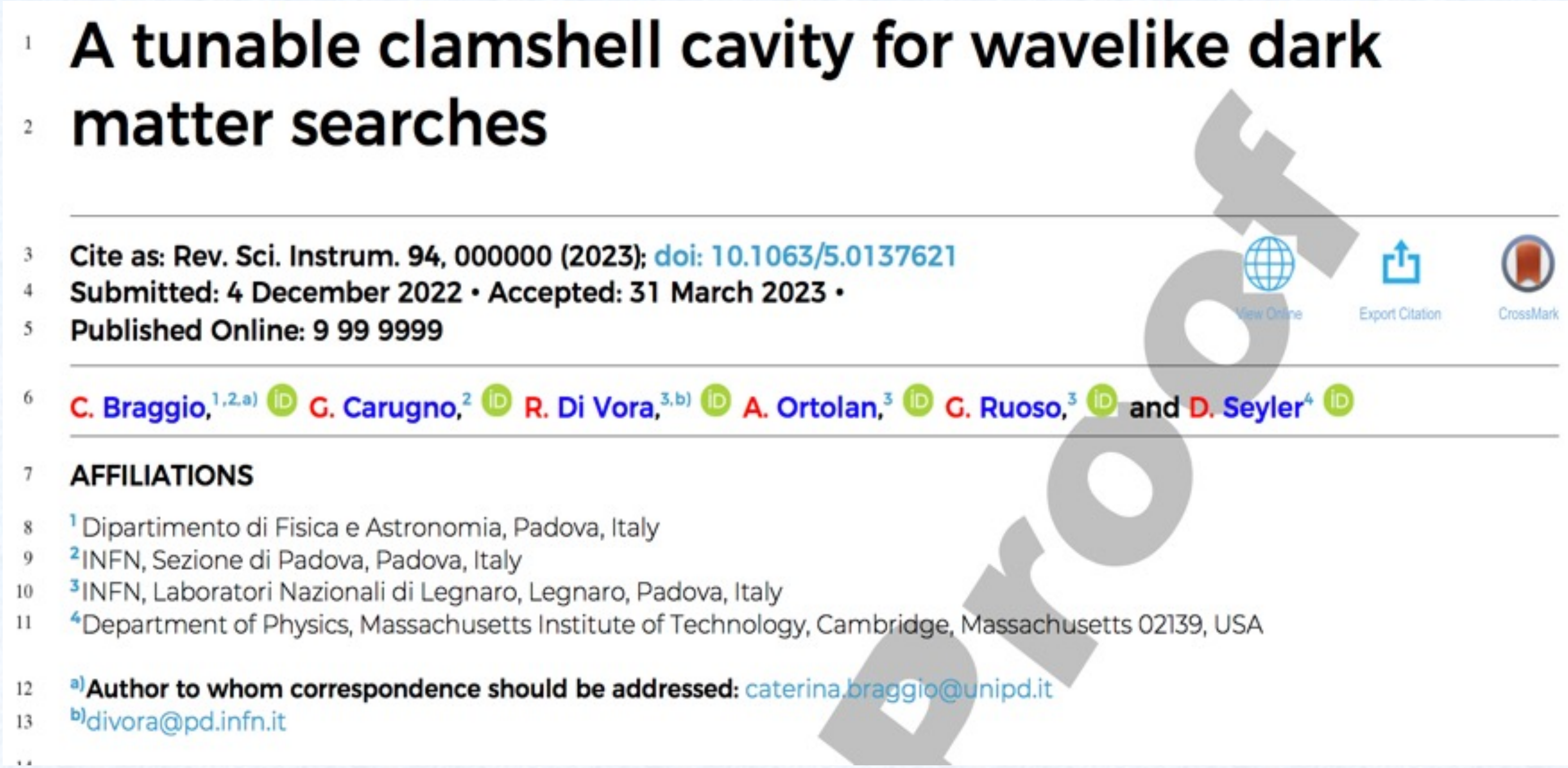

A tunable clamshell cavity for wavelike dark matter searches

Cite as: Rev. Sci. Instrum. 94, 000000 (2023); doi: 10.1063/5.0137621
Submitted: 4 December 2022 • Accepted: 31 March 2023 •
Published Online: 9 99 9999

C. Braggio,[1,2,a)] G. Carugno,[2] R. Di Vora,[3,b)] A. Ortolan,[3] G. Ruoso,[3] and D. Seyler[4]

AFFILIATIONS

[1] Dipartimento di Fisica e Astronomia, Padova, Italy
[2] INFN, Sezione di Padova, Padova, Italy
[3] INFN, Laboratori Nazionali di Legnaro, Legnaro, Padova, Italy
[4] Department of Physics, Massachusetts Institute of Technology, Cambridge, Massachusetts 02139, USA

a) Author to whom correspondence should be addressed: caterina.braggio@unipd.it
b) divora@pd.infn.it

Microwave Receivers: HEMT, JPA, TWPA, SMPD

- We started with **low noise linear amplifier**
- From **Low Noise Factory**

HEMT
High Electron
Mobility
Transistor

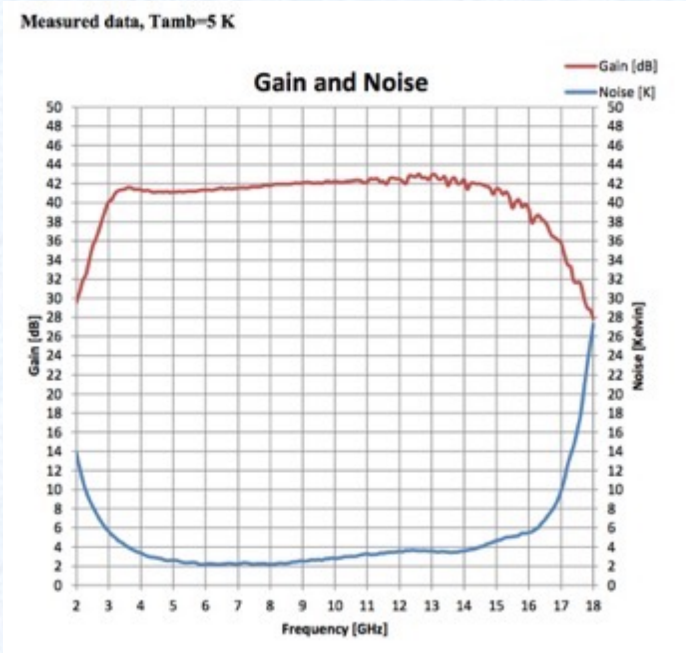

@ 14 GHz
@ 5 K

T_n = 4 K

Amplifier noise Temperature @ 5 K

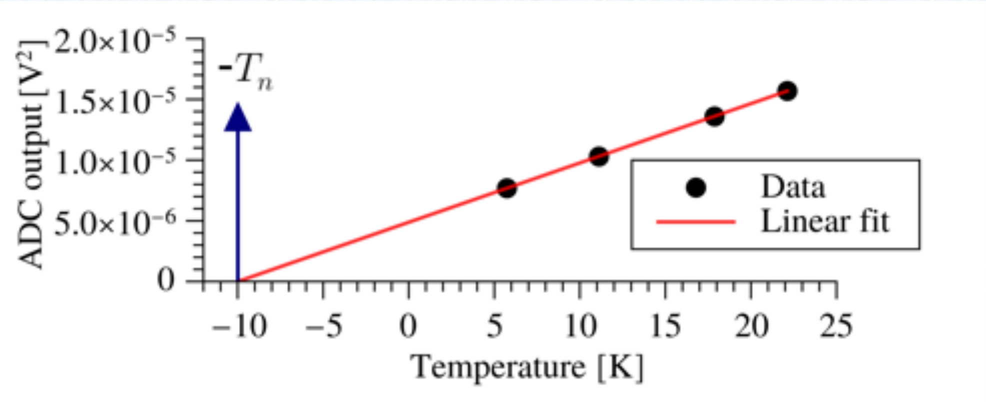

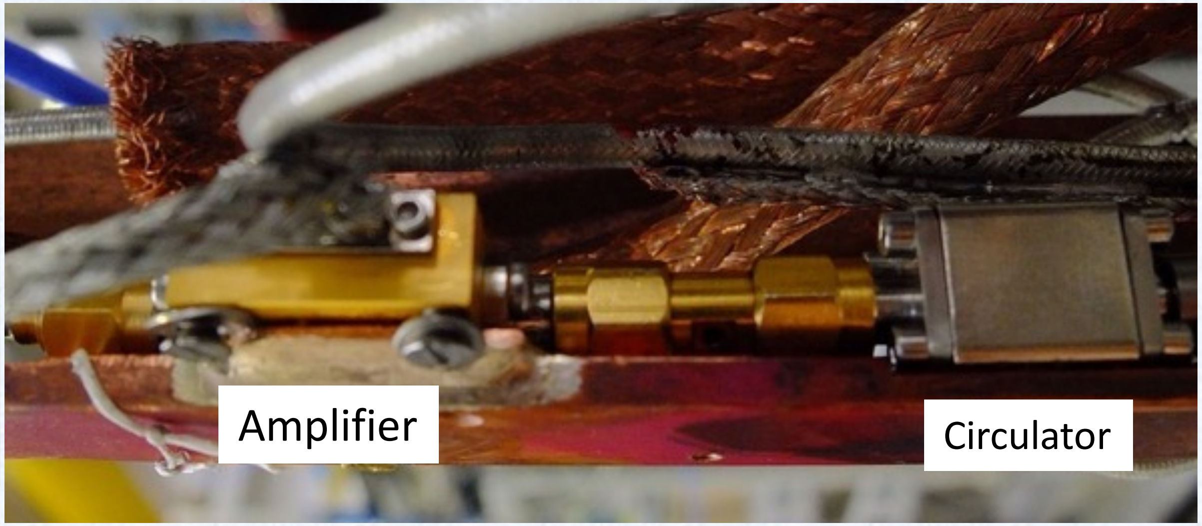

Noise Contributions @ Quantum Limit

System noise $\rightarrow$ thermal noise + quantum noise + added noise:

$$P_{noise}(\Delta\nu) = N(\nu, T) h\nu \Delta\nu = \left[\left(\frac{h\nu}{e^{\frac{h\nu}{k_B T}} - 1} \right) + h\nu \left(\frac{1}{2} + N_A \right) \right] \Delta\nu = k_B T_{sys} \Delta\nu$$

But: $h\nu \sim 0.5$ K at 10 GHz, T$\sim$ 0.1 K for our apparatus $\rightarrow$ only small contribution from the physical temperature
Let us then suppose $T_{sys} \approx T + T_A \sim 2$ K and $\Delta\nu \approx 8.6$ kHz:

$$P_{noise} \approx k_B T_s \Delta\nu \approx 2.4 \cdot 10^{-19}\, W$$

Then, from the Dicke radiometer equation, the fluctuations after Δt total integration time are:

$$\sigma_{Dicke} \sim k_B T_s \sqrt{\frac{\Delta\nu}{\Delta t}} = 4.2 \cdot 10^{-23}\, W \left(\frac{T_{sys}}{2\, K} \right) \left(\frac{\Delta\nu}{8.6\, kHz} \right)^{\frac{1}{2}} \left(\frac{3600\, s}{\Delta t} \right)^{\frac{1}{2}}$$

System Noise vs Scan Rate

We can better evaluate the performance of an haloscope by looking at its expected scan rate:

$$\frac{df}{dt} = \frac{1}{SNR^2}\left(\frac{P_0}{k_B T_{sys}}\right)^2 \left(\frac{\frac{\beta}{1+\beta}}{\frac{4\beta}{(1+\beta)^2}+\lambda}\right)^2 \left(\frac{Q_L Q_a}{Q_L + Q_a}\right)^2 ,$$

where $P_0 = g^2_{a\gamma\gamma}(\rho_a/m_a)B_0^2 V C_{mnl}$, $\lambda = T_A/T$ is the relative added noise contribution from outside the cavity and we defined the Signal-to-Noise Ratio (SNR) level of our scan as

$$SNR = \frac{P_{axion}}{\sigma_{Dicke}} = \frac{P_{axion}}{k_B T_{sys}}\sqrt{\frac{\Delta t}{\Delta\nu}} ,$$

By isolating the cavity-related factors we can then obtain the so-called cavity factor of merit F, which is very useful in designing cavities:

$$F = C^2_{mnl} V^2 \left(\frac{Q_0\, Q_a}{Q_0 + Q_a(1+\beta)}\right)^2 .$$

In the $Q_0 \sim Q_a$ regime and under the simplifying assumption $\beta \sim \beta_{opt} = 2$, we notice that this scales as Q_0

Josephson Parametric Amplifier @ Quantum Limit

- Acquired a commercial JPA (Josephson Parametric Amplifier)
  Quantum Circuits model JOC – Yale Spin-off company

- The amplification process arises from the dispersive nonlinearity of Josephson junctions driven with appropriate tones

- Signal (or idler) amplification only on a limited bandwidth

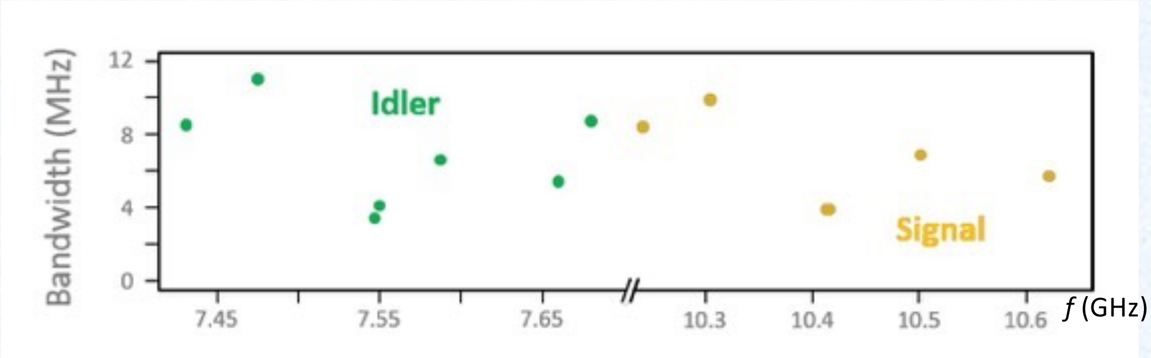

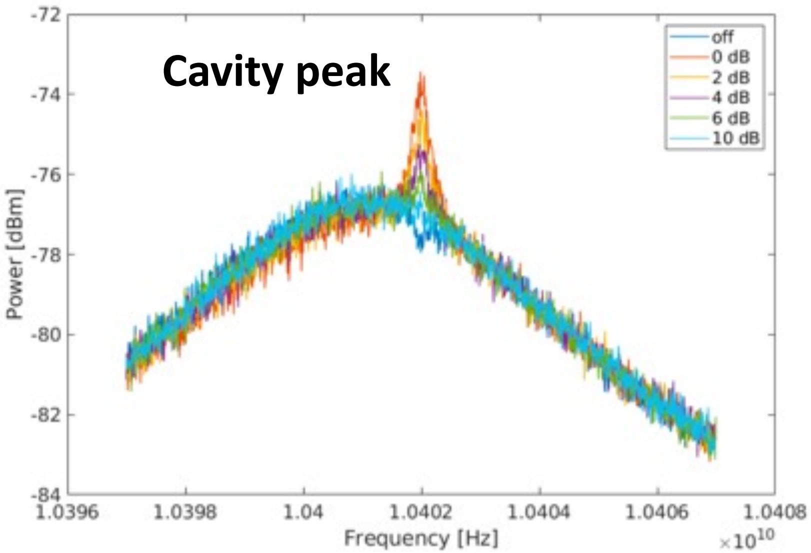

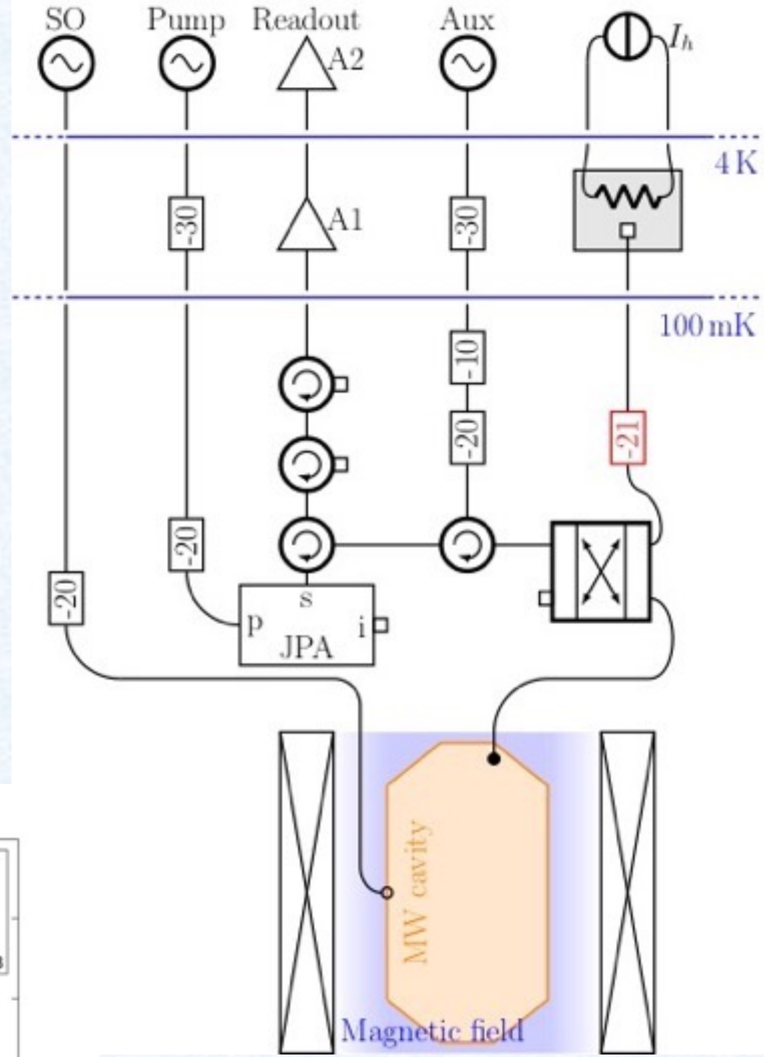

Gain curve of JPA @ 150 mK

- **Quantum limited linear amplifier**

- **@ *f* = 10 GHz ➔**
  $T_n \sim h f / k_B \sim 0.5$ K

Traveling Wave Parametric Amplifier Set-up

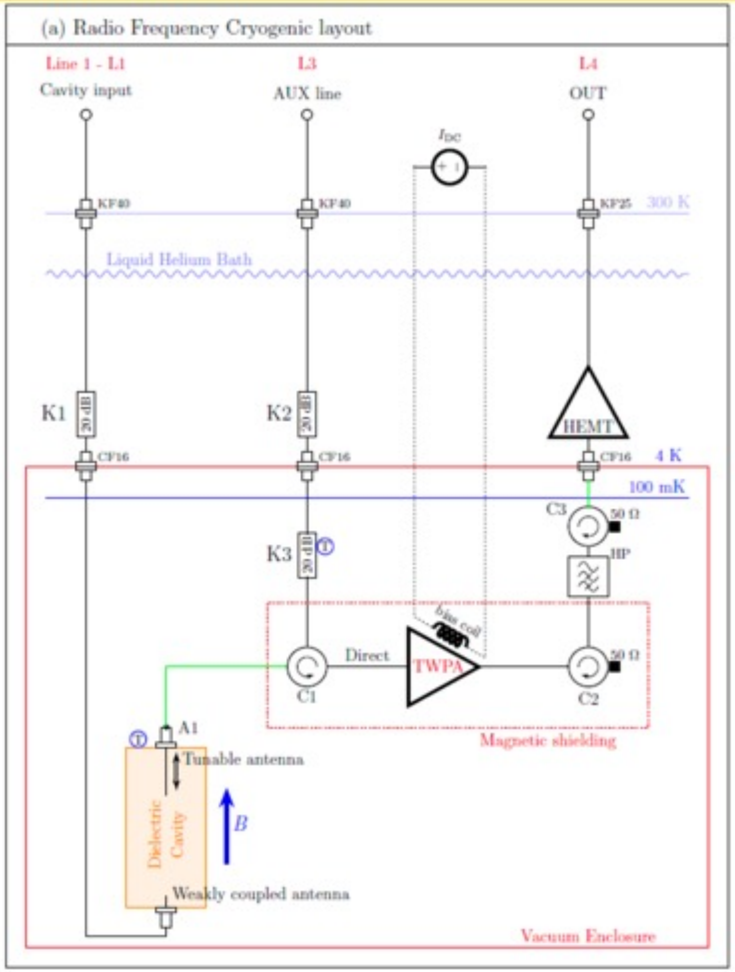

Cryostat TWPA Set-up

Picture of the cryogenic part of the receiver prior to TWPA installation

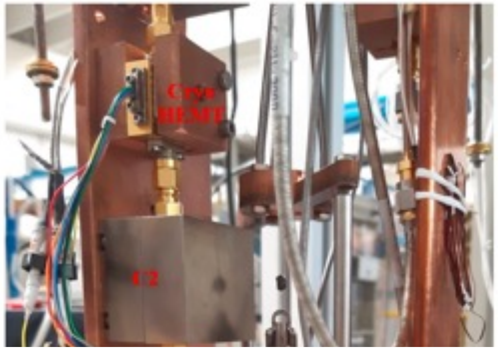

Room Temperature

RF Control Lines

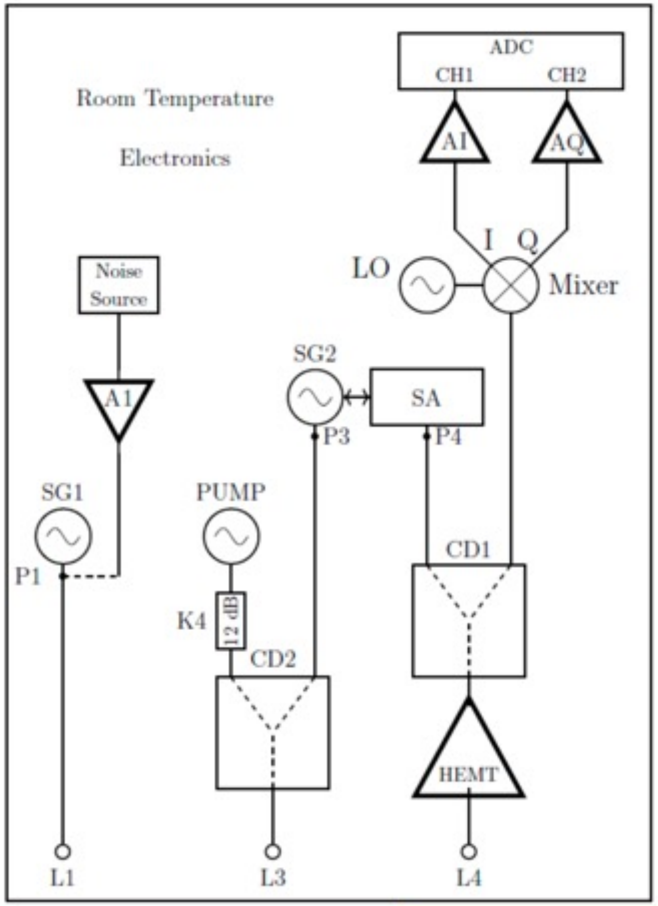

- Piloting the external source SG2 with the Spectrum Analyzer allows to obtain cavity parameters from reflection fit of **S43** (i.e. input on line 3, output on line 4) → ν_{cav}, Q_L, β
- The amplified 10^4 K diode noise source allows to obtain indipendent measurement of ν_{cav} and Q_L from **S41**
- SG2 also allows to add off-resonance monochromatic tone to monitor gain stability during data runs
- Data acquisition during runs handled by ADC
- All instruments referenced to GPS-disciplined clock

Traveling Wave Parametric Amplifier Results 1

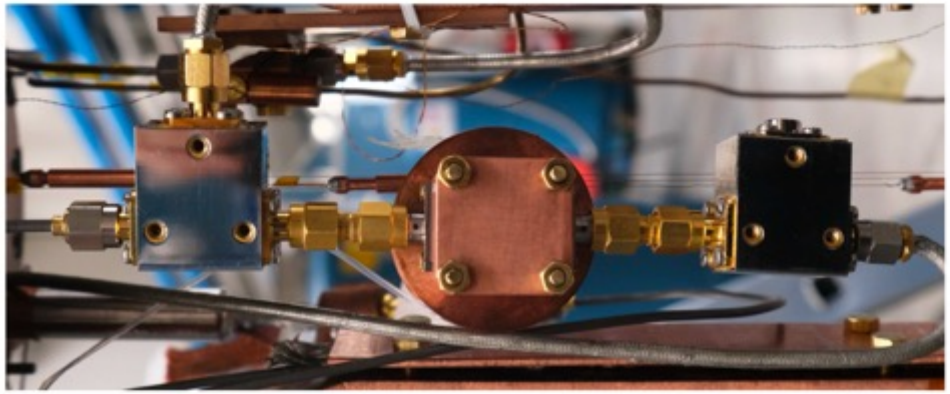

- Provided by Grenoble INP group **N.Roch group**
- Based on three-wave mixing, provides extremely wide-bandwidth amplification
- Tested repeatedly to ensure temporal stability and effective magnetic shielding
- Minimum T_{sys} obtained on frequency-tunable $\sim$ 1 MHz-wide maximum gain lobes

n	Magnetic field (T)	Cavity Temp. (K)	T_{sys} (K) On Res.	K3 Temp. (K)	T_{sys} (K) Off Res.
1	0	0.12	2.12 ± 0.05	0.18	2.22 ± 0.06
2	0	0.12	2.04 ± 0.03	0.19	1.94 ± 0.03
3	4.0	0.13	2.11 ± 0.03	0.22	2.16 ± 0.03
4	0	0.12	1.89 ± 0.04	0.18	1.98 ± 0.05
5	8.0	0.11	2.23 ± 0.06	0.18	2.26 ± 0.06

→ previous model described in 10.1063/5.0098039

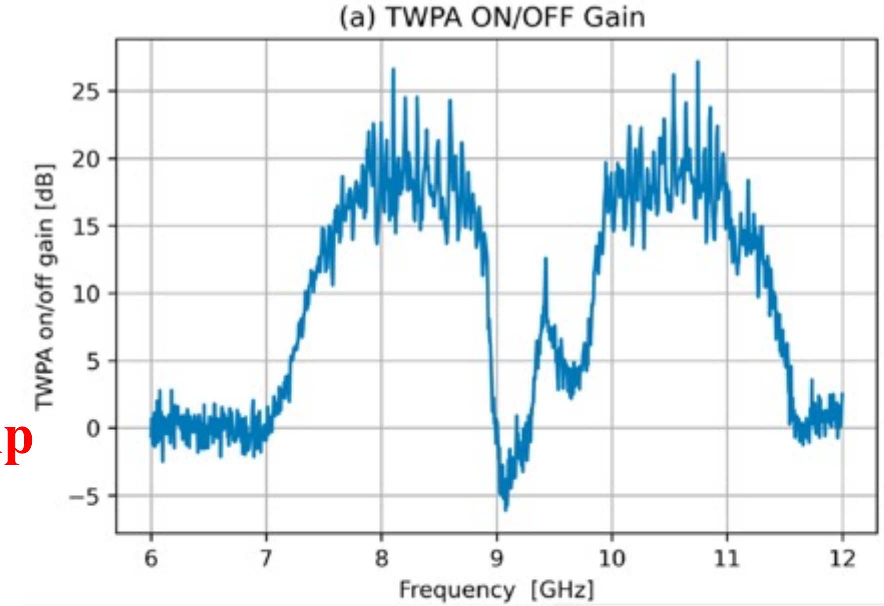

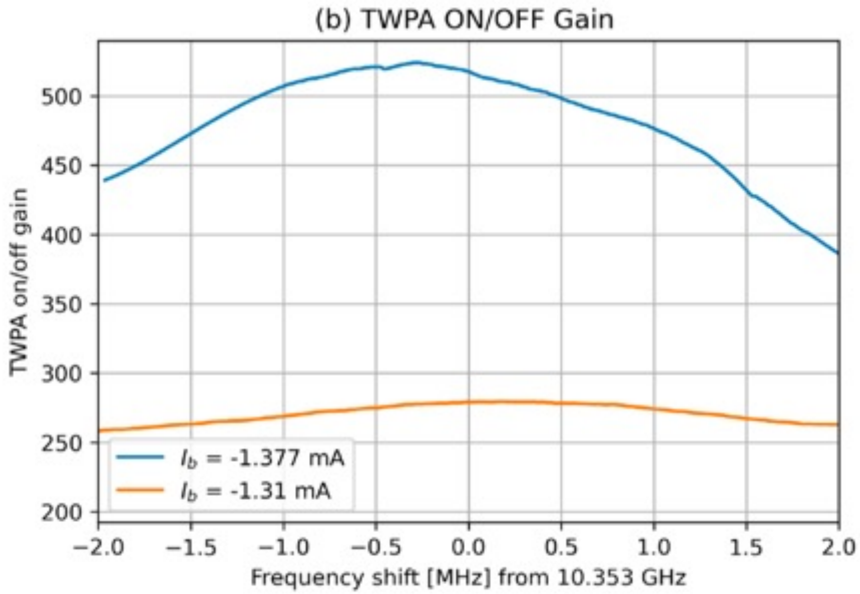

Traveling Wave Parametric Amplifier Results 2

The calibration procedure exploits the presence of three lines and is a two step process:

- First we calibrate the transmission G of the lines (the K are the VNA transmission measurement results):

$$\begin{cases} G_1 = \frac{K_{41}+K_{13}-K_{43}}{2} \\ G_3 = \frac{-K_{41}+K_{13}+K_{43}}{2} \\ G_4 = \frac{K_{41}-K_{13}+K_{43}}{2} \end{cases} \rightarrow \begin{cases} G_1 = (-74.7 \pm 0.1)\, dB \\ G_3 = (-50.9 \pm 0.1)\, dB \\ G_4 = (+52.1 \pm 0.1)\, dB \end{cases}$$

- Secondly we measure the noise level at the cavity tunable antenna through the Y-factor method:

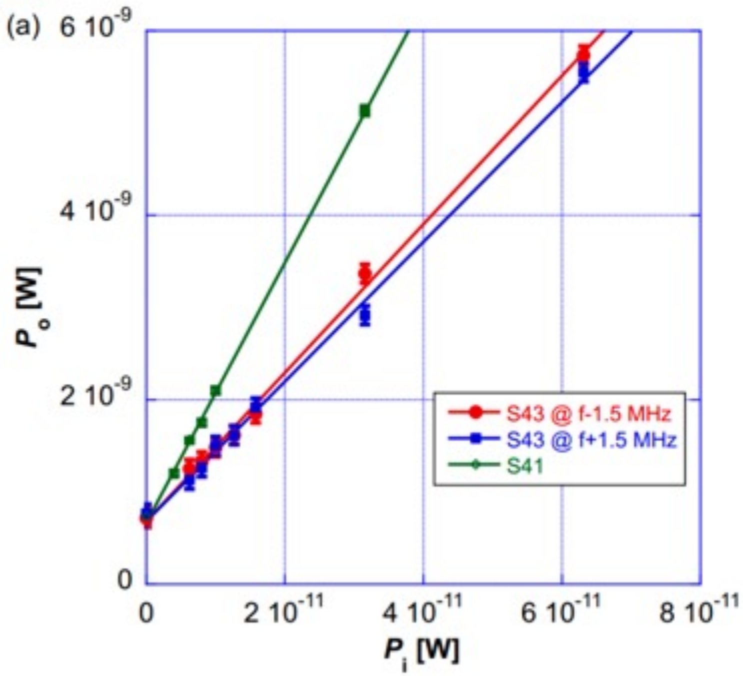

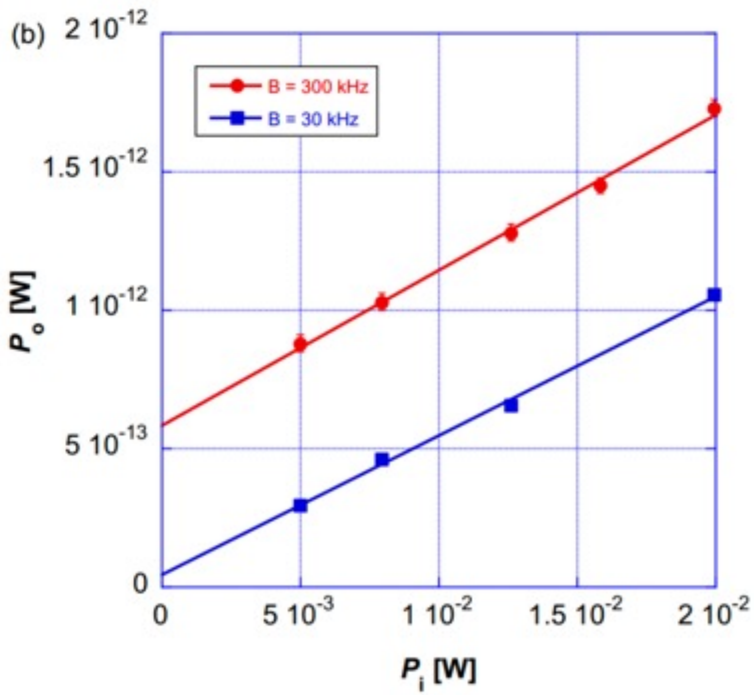

Traveling Wave Parametric Amplifier Results 3

We have $T_{sys}^{avg} = 2.06 \pm 0.13$ K on resonance, and $T_{sys}^{avg} = 2.07 \pm 0.14$ K off resonance.

Errors dominated by spread of the points → significant long term temperature variations

Noise contributions modeled at the HEMT output in the following general way:

$$PSD_{HEMT}(\nu_s) = h\nu_s G_{HEMT}[N_{HEMT} + (1-\Lambda_2)N_2 + \Lambda_2 G_{TWPA}(N_{TWPA}$$

$$+(1-\Lambda_1)N_1 + \Lambda_1 N(\nu_s; T_s) + \Lambda_1 N(\nu_i; T_i))]$$

We know the transmissions $\Lambda_{1,2}$ of the non-superconductive cables to be almost 1, and G_{HEMT} to be high; then, at the input point (3-wave mixing → the idler also adds noise):

$$N_{sys} \simeq N(\nu_s, T_s) + N(\nu_i, T_i) + \frac{N_{TWPA}}{\Lambda_1} + \frac{N_{HEMT}}{\Lambda_1 \Lambda_2 G_{TWPA}}$$

where N_{HEMT} can be estimated from the noise temperature of the system with TWPA off.

Term	Value (K)	N photons
$N(\nu_s, T_s)$	0.27	0.5
$N(\nu_i, T_i)$	0.27	0.7
$N_{\mathrm{HEMT}}/\Lambda_1\Lambda_2 G_{\mathrm{TWPA}}$	0.39	0.8
N_{sys}	2.06	4.2
$N_{\mathrm{TWPA}}/\Lambda_1$		2.2

Traveling Wave Parametric Amplifier Results 4

Review of Scientific Instruments ARTICLE scitation.org/journal/rsi

A haloscope amplification chain based on a traveling wave parametric amplifier

Cite as: Rev. Sci. Instrum. 93, 094701 (2022); doi: 10.1063/5.0098039
Submitted: 4 May 2022 • Accepted: 28 July 2022 •
Published Online: 6 September 2022

View Online Export Citation CrossMark

Caterina Braggio,[1,2] Giulio Cappelli,[3] Giovanni Carugno,[2] Nicolò Crescini,[3] Raffaele Di Vora,[2,4] Martina Esposito,[3,5] Antonello Ortolan,[6] Luca Planat,[3] Arpit Ranadive,[3] Nicolas Roch,[3] and Giuseppe Ruoso[6,a)]

AFFILIATIONS

[1] Dip. di Fisica e Astronomia, Università di Padova, 35100 Padova, Italy
[2] INFN - Sezione di Padova, 35100 Padova, Italy
[3] Univ. Grenoble Alpes, CNRS, Grenoble INP, Institut Néel, 38000 Grenoble, France
[4] Dip. di Scienze Fisiche, della Terra e dell'Ambiente, Università di Siena, 53100 Siena, Italy
[5] CNR-SPIN Complesso di Monte S. Angelo, Via Cintia, 80126 Napoli, Italy
[6] INFN - Laboratori Nazionali di Legnaro, 35020 Legnaro, Padova, Italy

[a)] **Author to whom correspondence should be addressed:** Giuseppe.Ruoso@lnl.infn.it

ABSTRACT

In this paper, we will describe the characterization of an RF amplification chain based on a traveling wave parametric amplifier. The detection chain is meant to be used for dark matter axion searches, and thus, it is coupled to a high Q microwave resonant cavity. A system noise temperature $T_{sys} = (3.3 \pm 0.1)$ K is measured at a frequency of 10.77 GHz, using a novel calibration scheme, allowing for measurement of T_{sys} exactly at the cavity output port.

Latest Results : QUAX-aγ search Run with TWPA

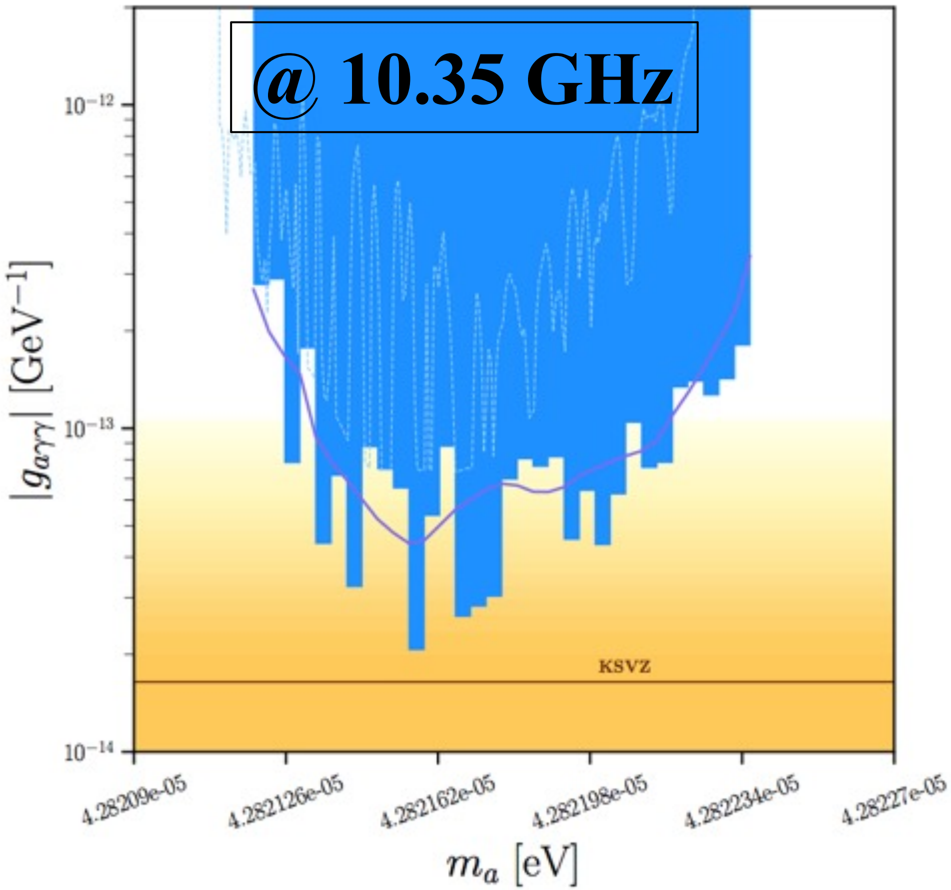

Search for galactic axions with a traveling wave parametric amplifier

R. Di Vora, A. Lombardi, A. Ortolan, R. Pengo, and G. Ruoso*
INFN, Laboratori Nazionali di Legnaro, 35020 Legnaro (Padova), Italy

C. Braggio
INFN, Sezione di Padova, 35100 Padova, Italy and
Dipartimento di Fisica e Astronomia, 35100 Padova, Italy

G. Carugno and L. Taffarello
INFN, Sezione di Padova, I-35100 Padova, Italy

G. Cappelli, N. Crescini, M. Esposito,† L. Planat, A. Ranadive, and N. Roch
Univ. Grenoble Alpes, CNRS, Grenoble INP, Institut Néel, 38000 Grenoble, France

D. Alesini, D. Babusci, A. D'Elia, D. Di Gioacchino, C. Gatti, C. Ligi, G. Maccarrone, A. Rettaroli, and S. Tocci
INFN, Laboratori Nazionali di Frascati, 00044 Frascati (Roma), Italy

D. D'Agostino, U. Gambardella, and G. Iannone
Dipartimento di Fisica E.R. Caianiello, 84084 Fisciano (Salerno), Italy and
INFN, Sezione di Napoli, 80126 Napoli, Italy

P. Falferi
Istituto di Fotonica e Nanotecnologie, CNR Fondazione Bruno Kessler, I-38123 Povo, Trento, Italy and
INFN, TIFPA, 38123 Povo (Trento), Italy

(QUAX Collaboration)

(Dated: April 13, 2023)

A traveling wave parametric amplifier has been integrated in the haloscope of the QUAX experiment. A search for dark matter axions has been performed with a high Q dielectric cavity immersed in a 8 T magnetic field and read by a detection chain having a system noise temperature of about 2.1 K at the frequency of 10.353 GHz. Scanning has been conducted by varying the cavity frequency using sapphire rods immersed into the cavity. At multiple operating frequencies, the sensitivity of the instrument was at the level of viable axion models.

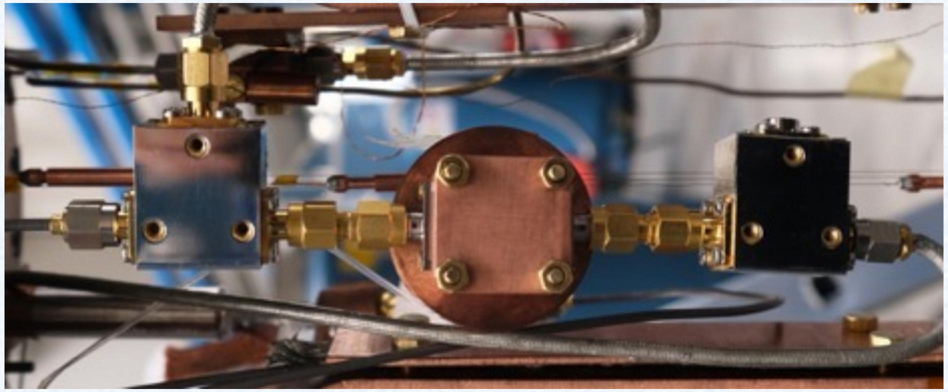

Run with high Q cavity @ 100 mK
8 T magnetic field
Tsys = 2,1 K (TWPA)

Ready To Start Scanning

QUAX-ae search Run with JPA

PHYSICAL REVIEW LETTERS **124,** 171801 (2020)

Axion Search with a Quantum-Limited Ferromagnetic Haloscope

N. Crescini,[1,2,*] D. Alesini,[3] C. Braggio,[2,4] G. Carugno,[2,4] D. D'Agostino,[5] D. Di Gioacchino,[3] P. Falferi,[6] U. Gambardella,[5] C. Gatti,[3] G. Iannone,[5] C. Ligi,[3] A. Lombardi,[1] A. Ortolan,[1] R. Pengo,[1] G. Ruoso,[1,†] and L. Taffarello[4]

(QUAX Collaboration)

[1]*INFN-Laboratori Nazionali di Legnaro, Viale dell'Università 2, 35020 Legnaro (PD), Italy*
[2]*Dipartimento di Fisica e Astronomia, Via Marzolo 8, 35131 Padova, Italy*
[3]*INFN-Laboratori Nazionali di Frascati, Via Enrico Fermi 40, 00044 Roma, Italy*
[4]*INFN-Sezione di Padova, Via Marzolo 8, 35131 Padova, Italy*
[5]*INFN-Sezione di Napoli, Via Cinthia, 80126 Napoli, Italy and Dipartimento di Fisica, Via Giovanni Paolo II 132, 84084 Fisciano (SA), Italy*
[6]*IFN-CNR, Fondazione Bruno Kessler, and INFN-TIFPA, Via alla Cascata 56, 38123 Povo (TN), Italy*

(Received 24 January 2020; revised manuscript received 12 March 2020; accepted 17 April 2020; published 1 May 2020)

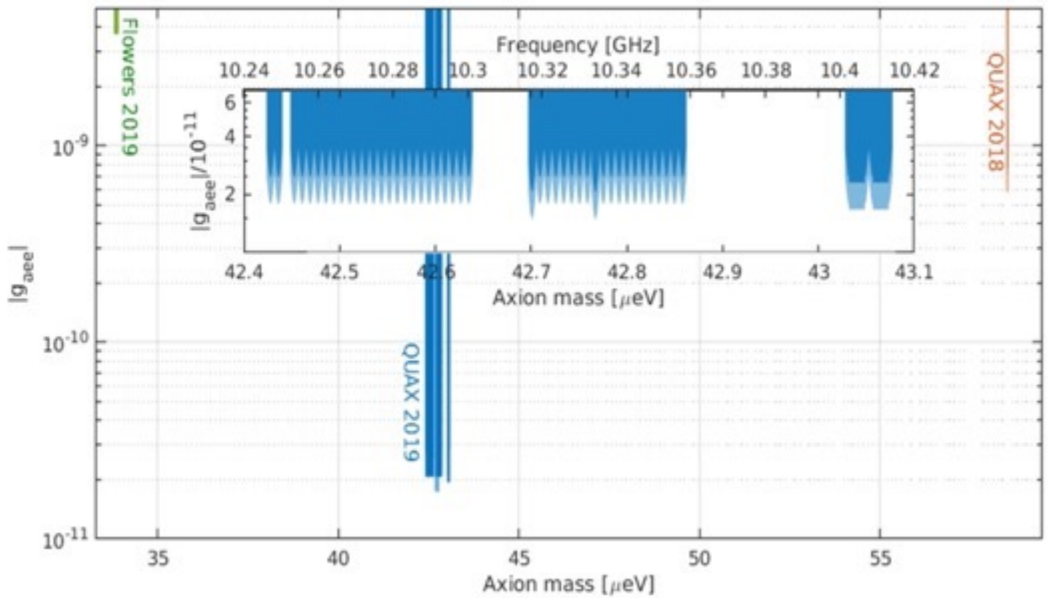

First operation of a ferrimagnetic haloscope with mass scanning through magnetic field tuning

Operating @ Quantum Limit ($B_{rf} = 10^{-19}$ Tesla)

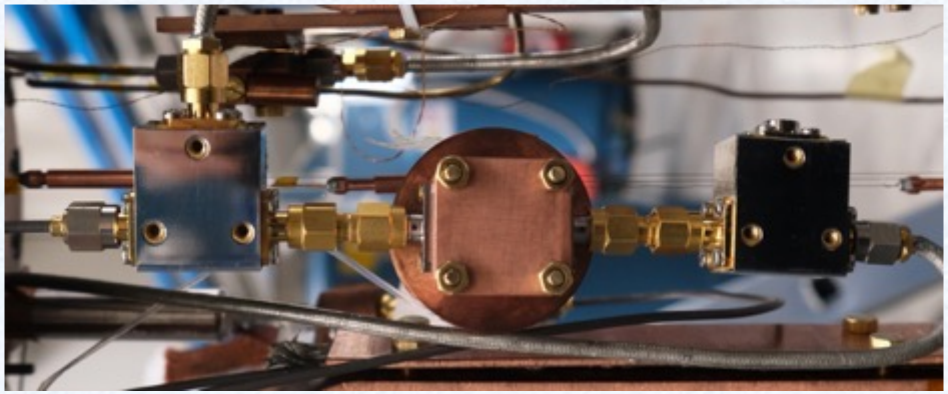

Run with high Q cavity @ 100 mK

0,5 T magnetic field

Tsys = 1 K (JPA) @ Quantum Limit

Cavity readout- Amplifier@SQL vs Photon Counter

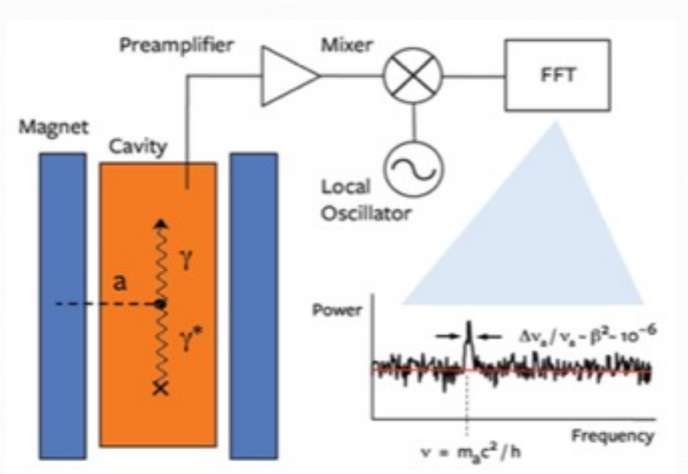

Dicke's receiver noise: fluctuations in the noise power within an integration time t_m over a frequency bandwidth Δν

$$\delta P_{\mathrm{n}} = \frac{P_{sys}}{\sqrt{t_m \Delta\nu}} \xrightarrow{T \to 0} k_B T_{eff} \sqrt{\frac{\Delta\nu}{t_m}}$$

$$k_B T_{eff} \xrightarrow{SQL} h\nu_a$$

$$P_a = 10^{-3} - 10^{-1} z \text{ Watt}$$

t_m=100 sec.
$\Delta\nu = 10^{-6}\,\nu_a$

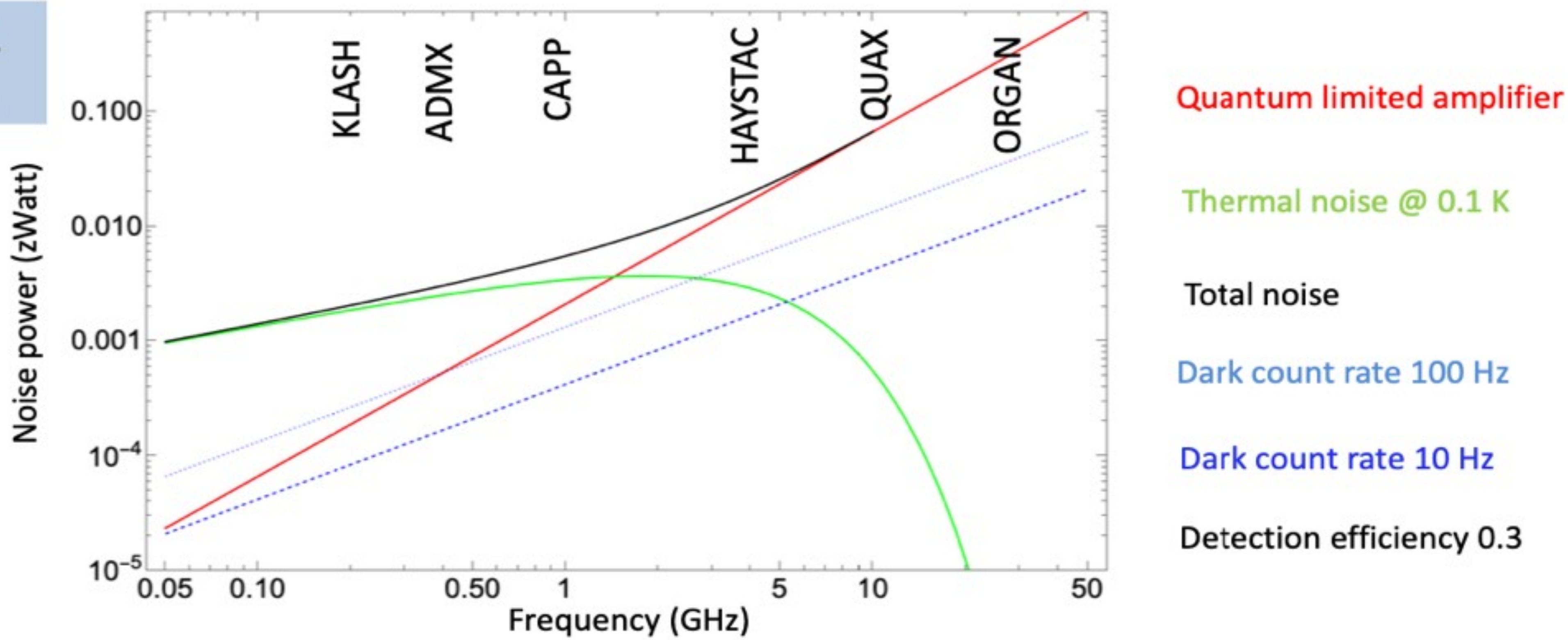

Beyond SQL ->Transmon Qubit

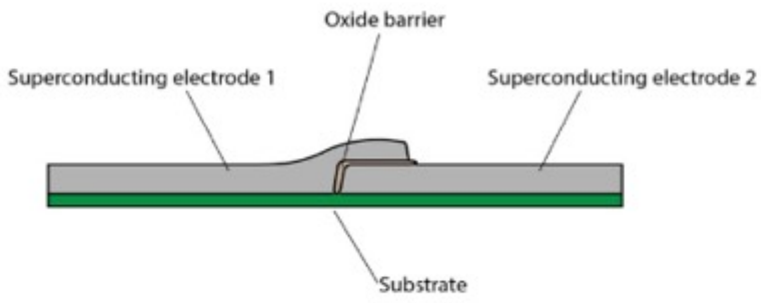

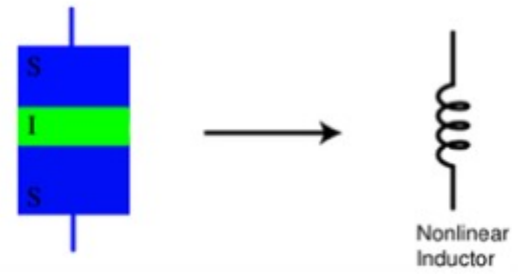

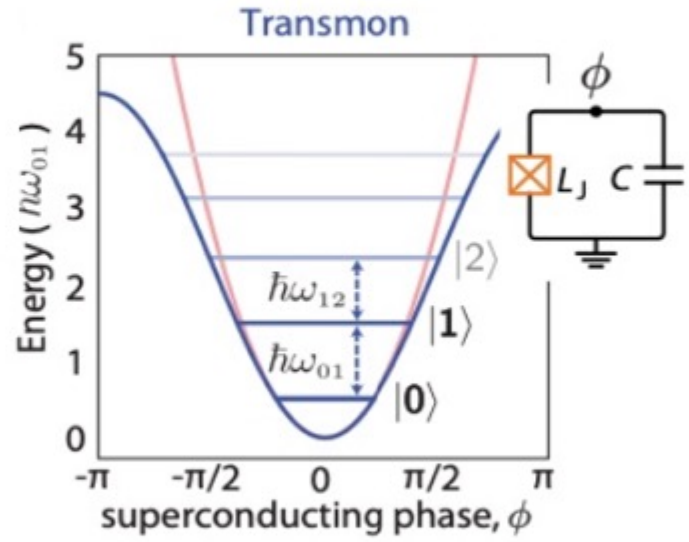

$\phi = \theta_1 - \theta_2$ Josephson phase

1st Josephson eq.: $I_J = I_c \sin\phi$ (DC)

2nd Josephson eq.: $V = \frac{\Phi_0}{2\pi}\frac{\partial\phi}{\partial t}$ (AC)

(DC) + (AC) → $V = \frac{\Phi_0}{2\pi}\frac{1}{I_c\cos\phi}\frac{\partial I_J}{\partial t} = L_J\frac{\partial I_J}{\partial t}$

·linear Josephson inductance: $L_J(\phi) = \frac{\Phi_0}{2\pi}\frac{1}{I_c\cos\phi}$

Harmonic & anharmonic oscillators → cQED

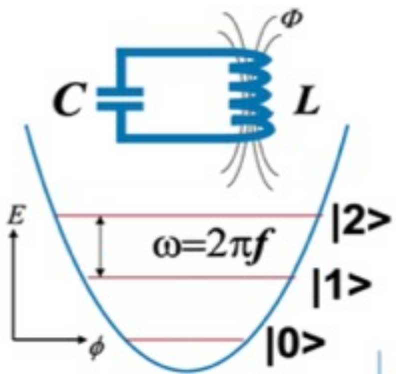

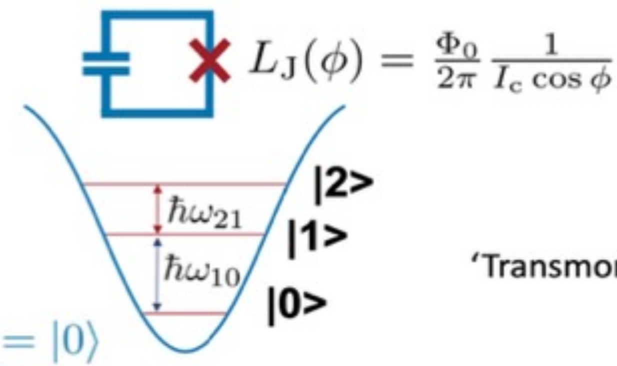

'Transmon

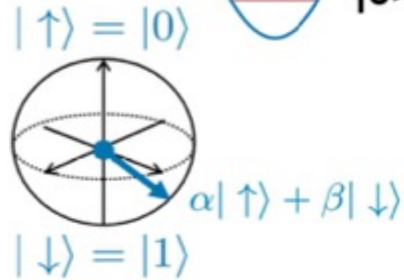

Figures: Courtesy of Martin Weides

M. Kjaergaard, et al Ann. Rev. Cond. Matt. Phys. **11**, 369-395 (2020)

Single Photon Microwave Detector

Detection of quantum microwaves

The detection of individual **microwave photons** has been pioneered by **atomic cavity quantum electrodynamics experiments** and later on transposed to **circuit QED experiments**

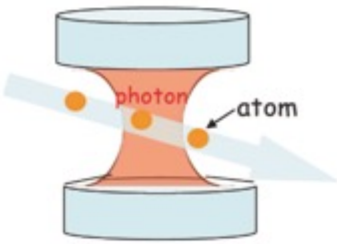

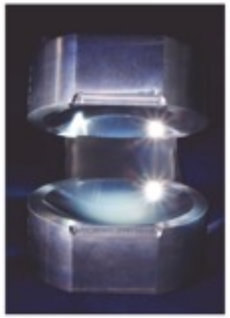

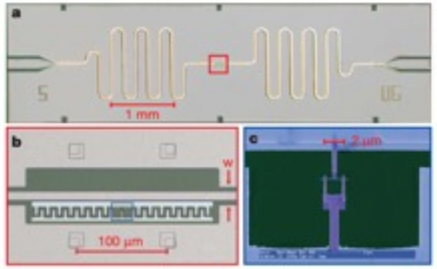

Nature **400**, 239–242 (1999)

Nature **445**, 515–518 (2007)

In both cases **two-level atoms** interact directly with a **microwave field mode*** in the cavity

* a quantum oscillator whose quanta are photons

from cavity-QED to circuit-QED

g is significantly increased compared to Rydberg atoms:

→ artificial atoms are large ($\sim 300\,\mu$m)
$\Longrightarrow$ large dipole moment

→ $\vec{E}$ can be tightly confined
$\vec{E} \propto \sqrt{1/\lambda^3}$
$\omega^2\lambda \approx 10^{-6}\,\mathrm{cm}^3$ (1D) versus $\lambda^3 \approx 1\,\mathrm{cm}^3$ (3D)
$\Longrightarrow 10^6$ larger energy density

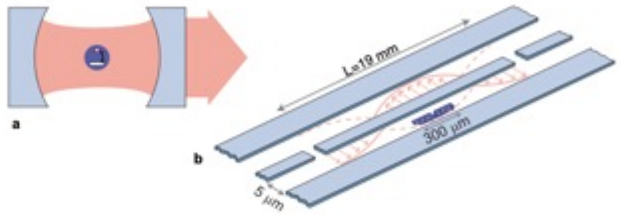

(a) $(g/2\pi)_{\mathrm{cavity}} \sim 50\,\mathrm{kHz}$

(b) $(g/2\pi)_{\mathrm{circuit}} \sim 100\,\mathrm{MHz}$ (typical)

10^4 larger coupling than in atomic systems

Single Photon Microwave Detector-1

In the Quantronics group (CEA, Saclay) a transmon-based counter has been developed and used to make spin fluorescence measurements, paving the way to **single spin flip detection** with SMPDs.

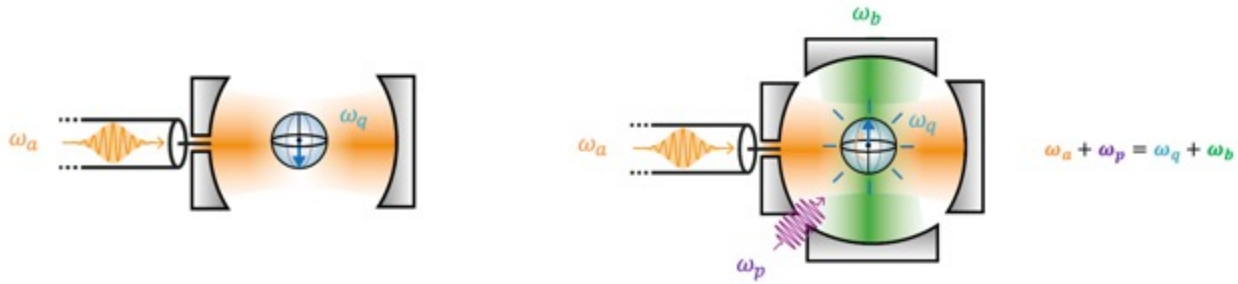

R. Lescanne *et al*, Phys. Rev. X 10, 021038 (2020)
E. Albertinale *et al*, Nature 600, 434 (2021)

Quantronics Group
Research Group in Quantum Electronics, CEA-Saclay, France

transmon-based SMPD

In the Quantronics group (CEA, Saclay) a transmon-based counter has been developed and used to make spin fluorescence measurements, paving the way to **single spin flip detection** with SMPDs.

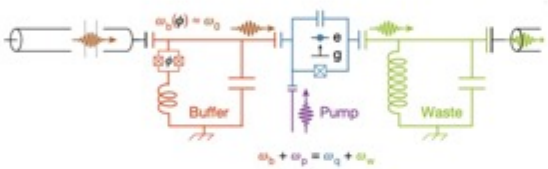

R. Lescanne *et al*, Phys. Rev. X 10, 021038 (2020)
E. Albertinale , Nature 600, 434 (2021)

Quantronics Group
Research Group in Quantum Electronics, CEA-Saclay, France

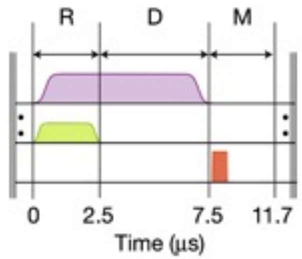

- a three-step process repeated several times
- qubit reset (R) performed by turning on the pump pulse + a weak resonant coherent pulse to the waste port
- detection (D) step with the pump pulse on
- measurement (M) step probes the dispersive shift of the buffer resonator to infer the qubit state

SMPD vs Haloscope Rate Expectation

	ν_c GHz	Q	β	B T	V cm^3	C_{nml}	$P_{a\gamma\gamma}$ 10^{-24}W	Γ_{sig} Hz
pilot exp.	7.3	4×10^5	1	3 T	113	0.64	0.95 (KSWZ)	0.2
							0.13 (DFSZ)	0.02
QUAX	10.48	1×10^6	1	14 T	1150	0.47	439 (KSWZ)	63
							60 (DFSZ)	8.7

- KSVZ $\longrightarrow$ DFSZ
- Photon counting is a game changer at high frequency and low temperatures: in the **energy eigenbasis** there is no intrinsic limit (SQL)

$$k_B T_{sys} = h\nu \left(\frac{1}{e^{h\nu/k_B T} - 1} + \frac{1}{2} + N_a \right)$$

- unlimited (exponential) gain in the haloscope scan rate compared to linear amplification at SQL:

$$\frac{R_{\text{counter}}}{R_{\text{SQL}}} \approx \frac{Q_L}{Q_a} e^{\frac{h\nu}{k_B T}}$$

at 7 GHz, 40 mK $\Longrightarrow$ 10^3 faster than SQL linear amplifier readout!

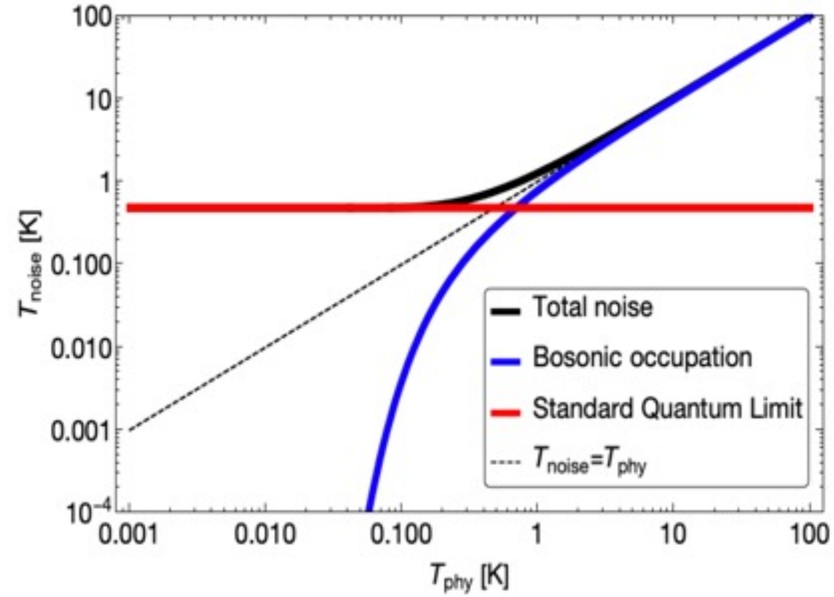

plot example at 10 GHz

SMPD vs Haloscope Rate Expectation

$\delta N_{dc} = \sqrt{\Gamma_{dc}\tau}$ uncertainty in the number of dark counts collected in an integration time τ

$\Sigma = \frac{\eta\Gamma_{sig}\tau}{\sqrt{\Gamma_{dc}\tau}} = \eta\Gamma_{sig}\sqrt{\frac{\tau}{\Gamma_{dc}}}$ the dark count contribution to the fluctuations dominates

$R_{\text{counter}} = \frac{\Delta\nu_c}{\tau} = \frac{\Delta\nu_c\eta^2 P^2_{a\gamma\gamma}}{h^2\nu^2\Sigma^2\Gamma_{dc}}$ $R_{\text{lin}} = \frac{Q_a}{Q_c}\left(\frac{P_{a\gamma\gamma}}{k_B T\sigma}\right)^2$ scan rates lin. amp. and counter

$$\frac{R_{\text{counter}}}{R_{\text{lin}}} = \left(\frac{k_B T_{sys}}{h\nu}\right)^2 \frac{\eta^2\Delta\nu_a}{\Gamma_{dc}}$$

quantum advantage can be demonstrated even with high dark count rates Γ_{dc}
$\eta \approx 0.4$, $\Gamma_{dc} \approx 100\,\text{Hz} \Longrightarrow$ potential improvement of a factor 11 compared to SQL scan rate

Pilot Experiment @ Saclay

PILOT SMPD-HALOSCOPE experiment

- copper cavity **sputtered with NbTi**
  magnetron sputtering in INFN-LNL
- right cylinder resonator, TM_{010} mode
  $\nu_c \sim 7.3\,\mathrm{GHz}$
- **system of sapphire triplets** to tune the cavity frequency
- T=14 mK delfridge base temperature
- **ultra-cryogenic nanopositioner** to change the sapphire rods position
- **3 T** (90 A) SC magnet
  (U. Gambardella, INFN Salerno)

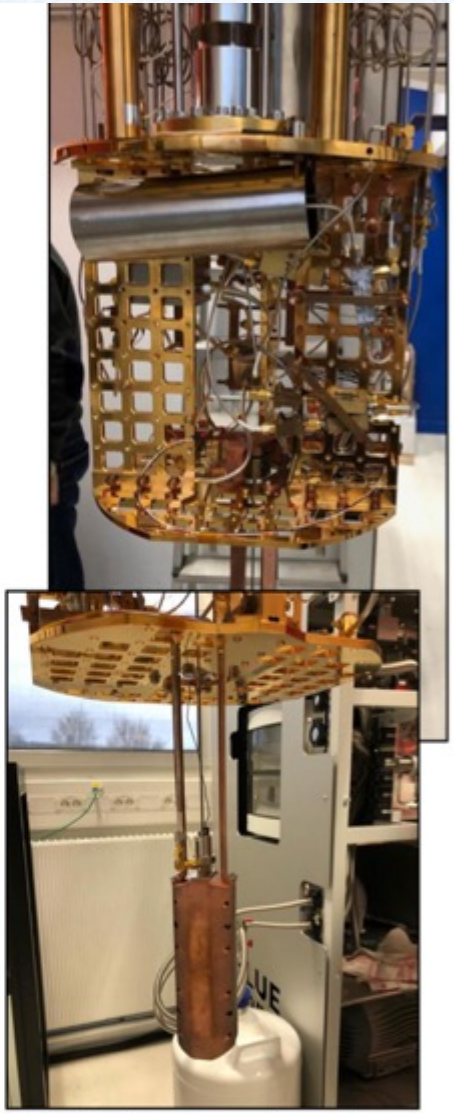

SMPD (top) and cavity

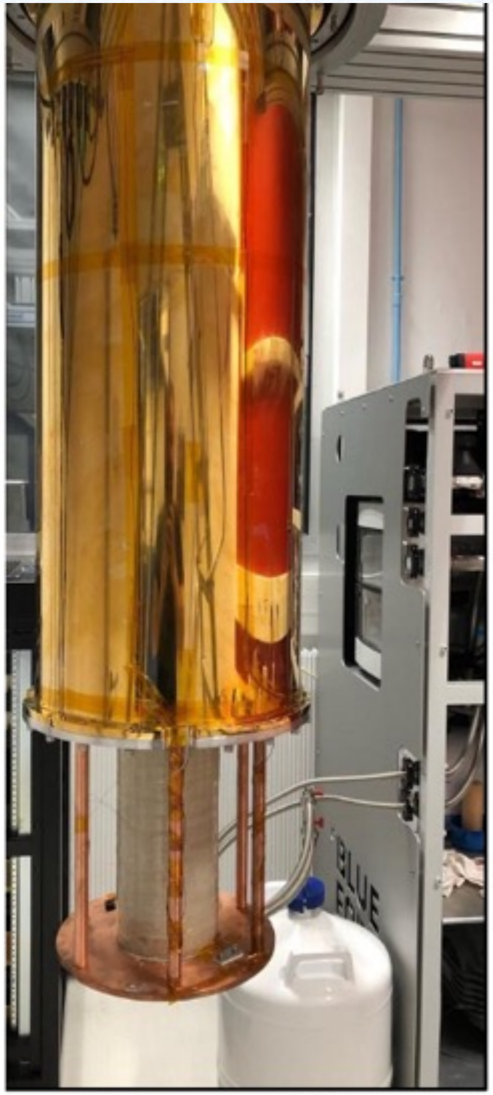

SC magnet

Haloscope Quantum Protocol: Cavity Tuning

In addition to recording clicks at the cavity frequency, the measurement protocol is devised so as to **continuously monitor** both **off-resonance counts** and the **SMPD efficiency while the cavity frequency is slowly varied**.

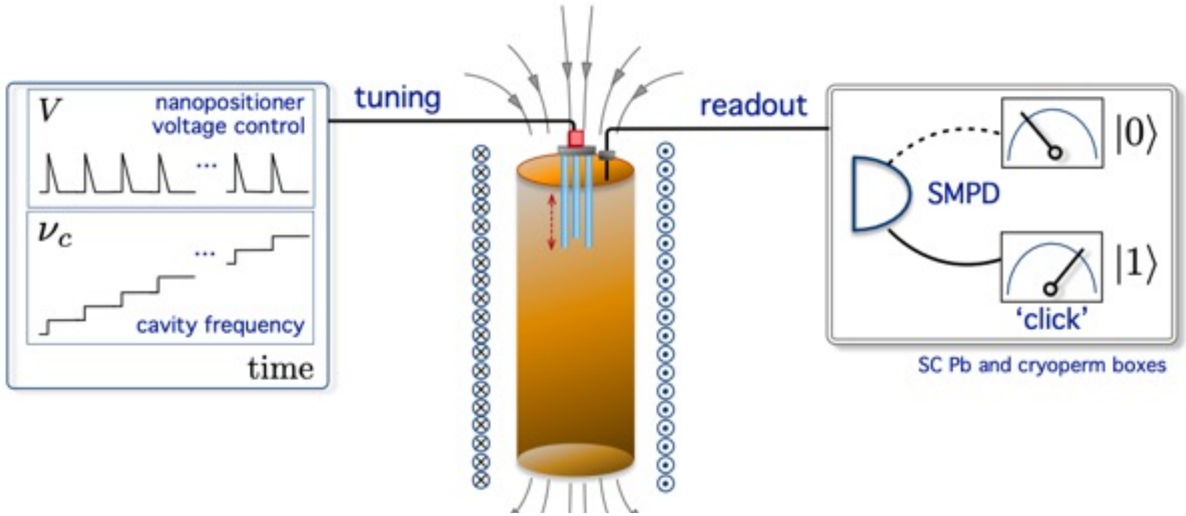

the dark counts arise from a non-homogeneous Poisson process: the average Γ_{DC} changes in time
$\Longrightarrow$ the **background must be constant in time** for haloscope search

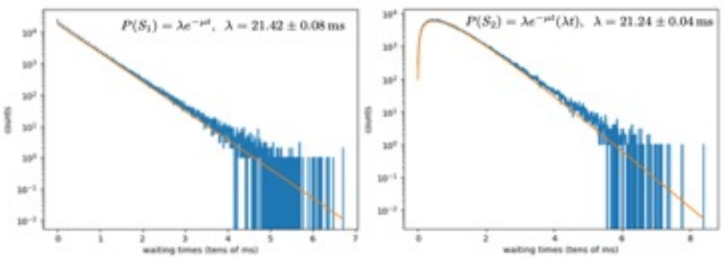

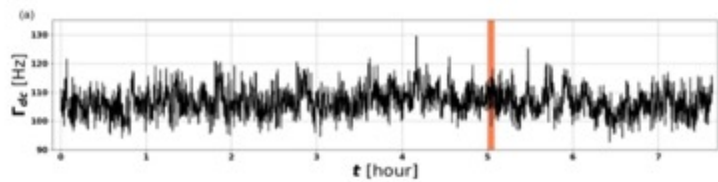

A solution is to **infer the noise** at cavity frequency **by continuously measuring the background** on sidebands

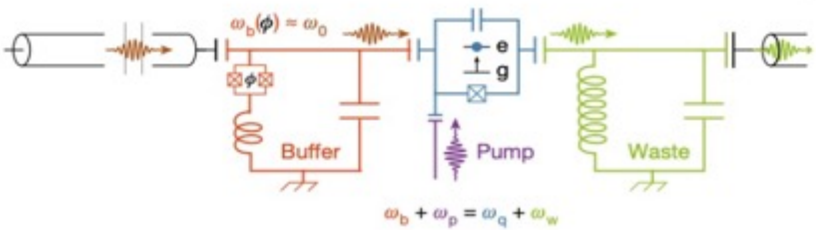

switching **SMPD readout frequency**
= buffer center frequency

→ tuned to cavity resonant frequency

→ detuned from cavity to infer noise Γ_{dc}

Haloscope Quantum Protocol: Efficiency vs Dark Count

In the measurement protocol counts at both the cavity frequency and at 4 sidebands frequencies are monitored **with a fixed input signal** from **a reference RF source** is sent at the buffer input = signal ON

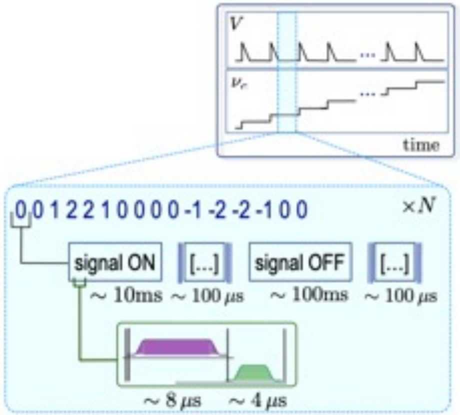

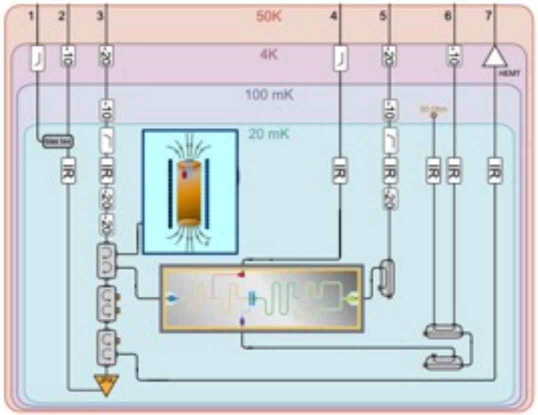

- 0 is buffer frequency at cavity resonance
- ±1, ±2 is same at $\nu_c \pm 1$, $\nu_c \pm 2\,\mathrm{MHz}$
- buffer resonator linewidth $\Delta f \sim 800\,\mathrm{kHz}$

In the measurement protocol counts at both the cavity frequency and at 4 sidebands frequencies are monitored **with no input signal at the buffer input**= signal OFF

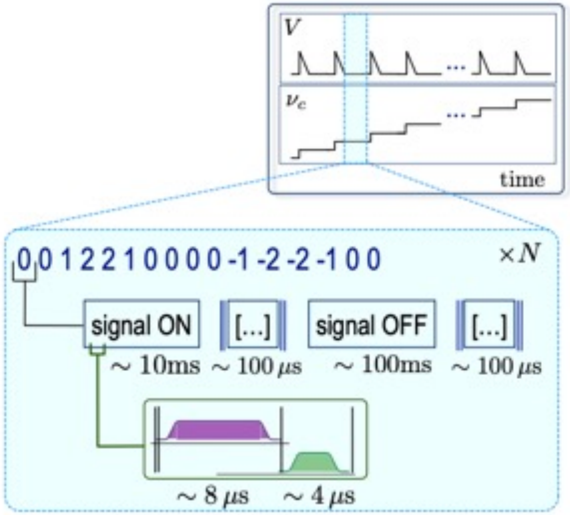

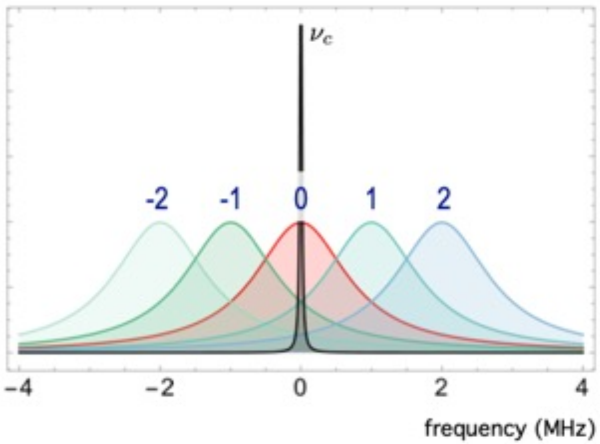

- 0 is buffer frequency at cavity resonance
- ±1, ±2 is same at $\nu_c \pm 1$, $\nu_c \pm 2\,\mathrm{MHz}$
- buffer resonator linewidth $\Delta f \sim 800\,\mathrm{kHz}$

Conclusions & Perspectives

1) Linear Josephson based Parametric Amplifier @ Quantum Limit in operation

2) Single Microwave Photon Detector (SMPD) are on the way to axion physics

3) Large target of polarized electrons matter vs single electron spin flip detection

4) SMPD open the route to other possible particles physics opportunities as:

   a) neutrino magnetic moment measurements through electron scattering

   b) spin dependent dark matter interactions

   c) Cosmic Microwave Background single photon detection (Hamburry-Brown Twiss)

- Back up slides

Interaction of DFSZ axion and electron spin

- The interaction of the DFSZ axion with a spin ½ particle

[redacted]

$$g_p \cong \frac{m_e}{3 f_a} \cos^2 \beta$$

$$g_p \approx 3 \times 10^{-11} \left(\frac{m_a}{1\, eV} \right)$$

- DFSZ axion coupling with non relativistic (v/c << 1) electron: equation of motion reduces to the Schroedinger equation

$$i\hbar \frac{\partial \varphi}{\partial t} = \left[-\frac{\hbar^2}{2m} \nabla^2 - \frac{g_p \hbar}{2m} \boldsymbol{\sigma} \cdot \boldsymbol{\nabla} a \right] \varphi$$

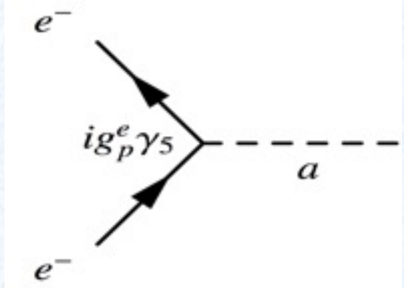

- Cold Dark Matter of the Universe may consists of axions and they can be searched for

The interaction term has the form of a **spin - magnetic field interaction** with $\vec{\nabla} a$ playing the role of an **oscillating effective magnetic field**

$$\mathrm{H}_{\mathrm{int}} = -2 \mu_B \vec{\sigma} \cdot \left[\frac{g_p}{2e} \vec{\nabla} a \right]$$

$$\mathrm{B}_a = \frac{g_p}{2e} \vec{\nabla} a$$

-- **Frequency** of the effective magnetic field proportional to **axion energy**
-- **Amplitude** of the effective magnetic field proportional to **axion density**

The axion wind

- **Due to the motion of the solar system** in the galaxy, the axion DM cloud acts as an **effective RF magnetic field on electron spin**
- RF field excites **magnetic transition in a magnetized sample** (Larmor frequency) with a static magnetic field $\mathbf{B_0}$ and can produces a detectable signal
- **The interaction with axion field produces a variation of magnetization which is in principle measurable**

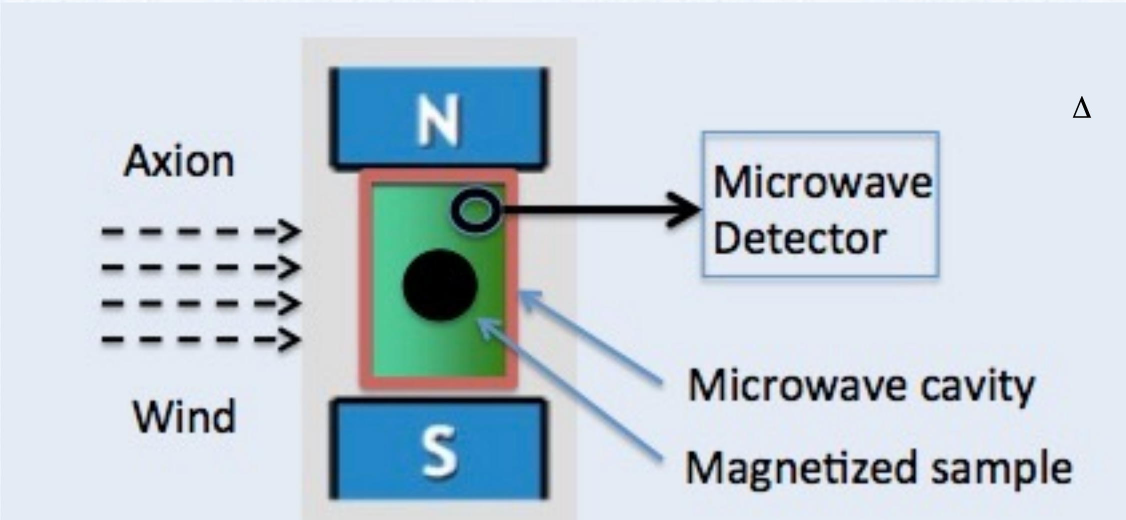

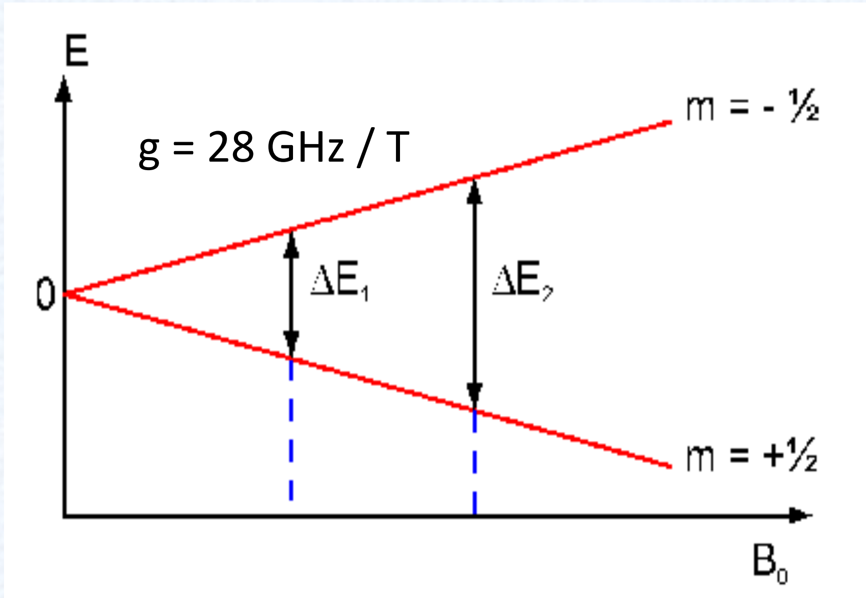

Idea is not new and comes from **several works**:

- L.M. Krauss, J. Moody, F. Wilczeck, D.E. Morris, "Spin coupled axion detections", HUTP-85/A006 (1985)
- R. Barbieri, M. Cerdonio, G. Fiorentini, S. Vitale, Phys. Lett. B 226, 357 (1989)
- F. Caspers, Y. Semertzidis, "Ferri-magnetic resonance, magnetostatic waves and open resonators for axion detection", Workshop on Cosmic Axions, World Scientific Pub. Co., Singapore, p. 173 (1990)
- A.I. Kakhizde, I. V. Kolokolov, Sov. Phys. JETP 72 598 (1991)

The axion effective magnetic field

- R. Barbieri et al., *Searching for galactic axions through magnetized media: The QUAX proposal* [Phys. Dark Univ. **15,** 135 - 141 (2017)]

The effective magnetic field associated with the axion wind

$$B_a = \frac{g_p}{2e}\left(\frac{n_a h}{m_a c}\right)^{1/2} m_a \mathrm{v}_E$$

n_a – axion density ∼ 0.4 Gev/cm^3
v_E – Earth velocity ∼220 km/s
axion velocity dispersion ∼270 km/s

Using from standard model of Galactic Halo:

$$B_a = 2.0 \cdot 10^{-22}\left(\frac{m_a}{200\,\mu\mathrm{eV}}\right)\ \mathrm{T},$$

$$\frac{\omega_a}{2\pi} = 48\left(\frac{m_a}{200\,\mu\mathrm{eV}}\right)\ \mathrm{GHz},$$

$$\tau_{\nabla a} \simeq 0.68\,\tau_a = 17\left(\frac{200\,\mu\mathrm{eV}}{m_a}\right)\left(\frac{Q_a}{1.9\times 10^6}\right)\ \mu\mathrm{s};$$

Coherence time

$$\lambda_{\nabla a} \simeq 0.74\,\lambda_a = 5.1\left(\frac{200\,\mu\mathrm{eV}}{m_a}\right)\ \mathrm{m},$$

Correlation length

Polarized matter: directional DM search

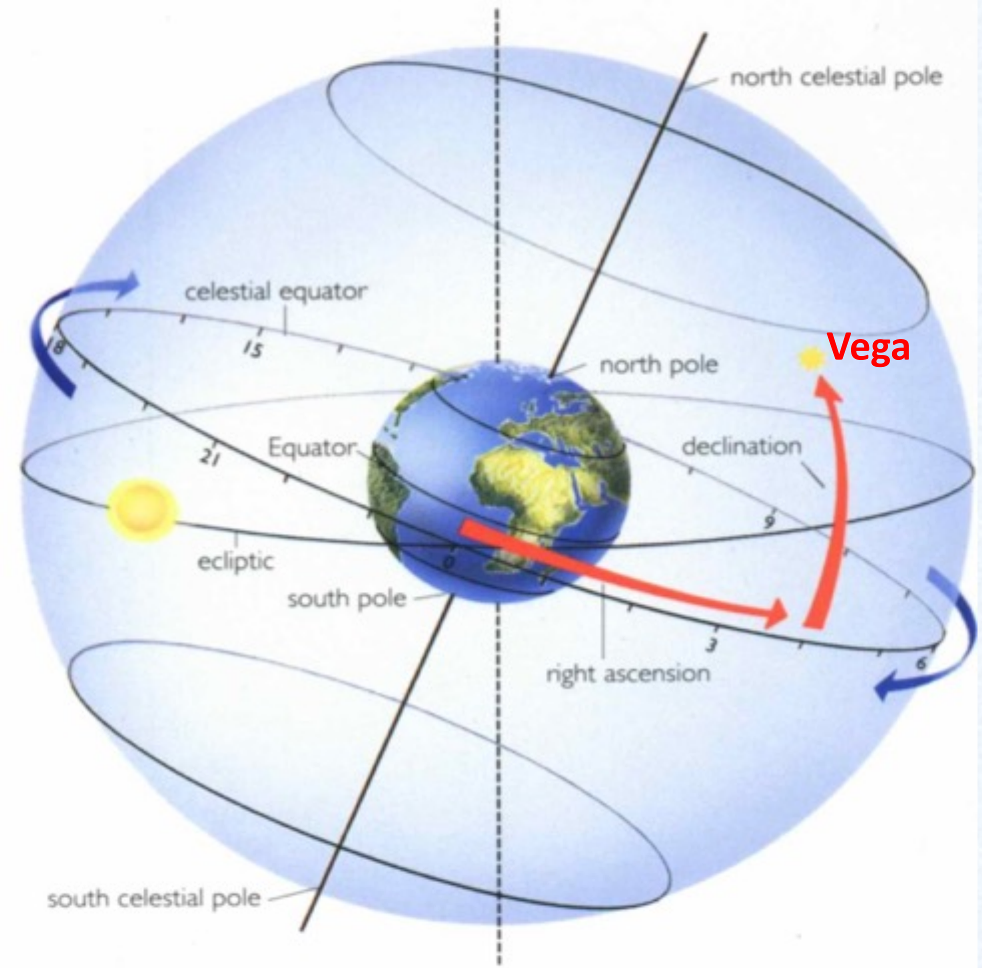

Due to Earth rotation, the direction of the static magnetic field $\mathbf{B_0}$ changes with respect to the direction of the axion wind (Vega in Cygnus)

e.g. QUAX located @Legnaro (PD)
$\mathbf{B}_0$ in the local horizontal plane and oriented N-S (the local meridian)

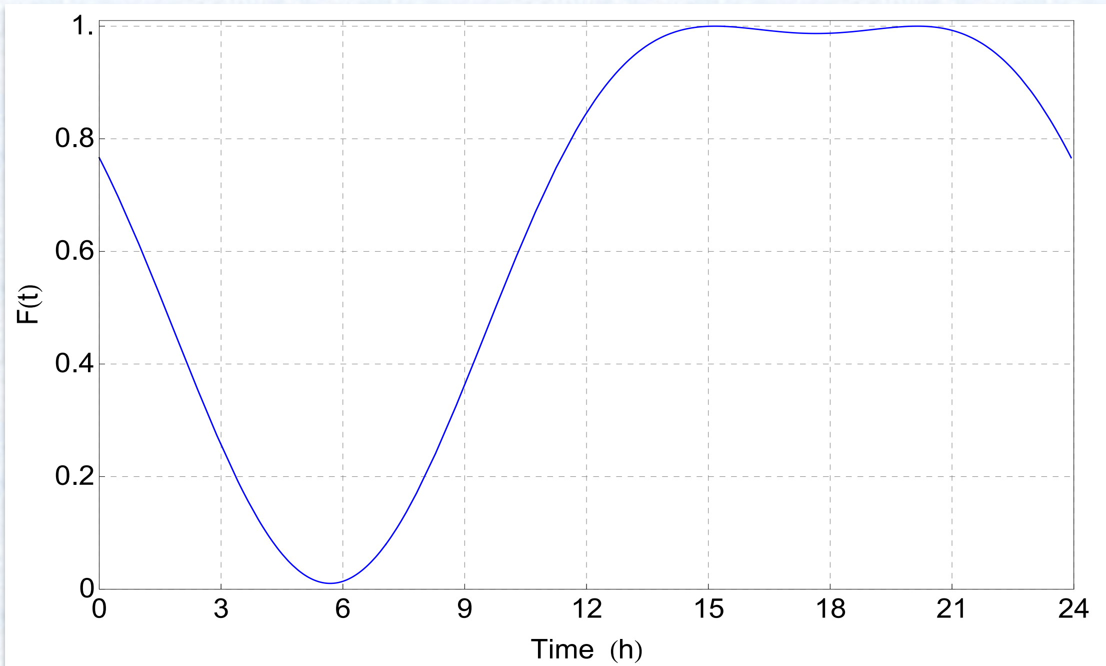

Strong modulation (up to 100%)!
Not due to seasonal or Earth rotation Doppler effect (few %) but to relative direction change of magnetic field respect to axion wind

Detection strategy: Electron Spin Resonance

Electron spin resonance (ESR) arises when energy levels of a quantized system of electronic moments are **Zeeman split** (the **magnetic system** is placed in a uniform magnetic field B_0) and the system absorbs/emits EM radiation (in the microwave range) at the **Larmor frequency n_L** of the **ferromagnetic resonance**.

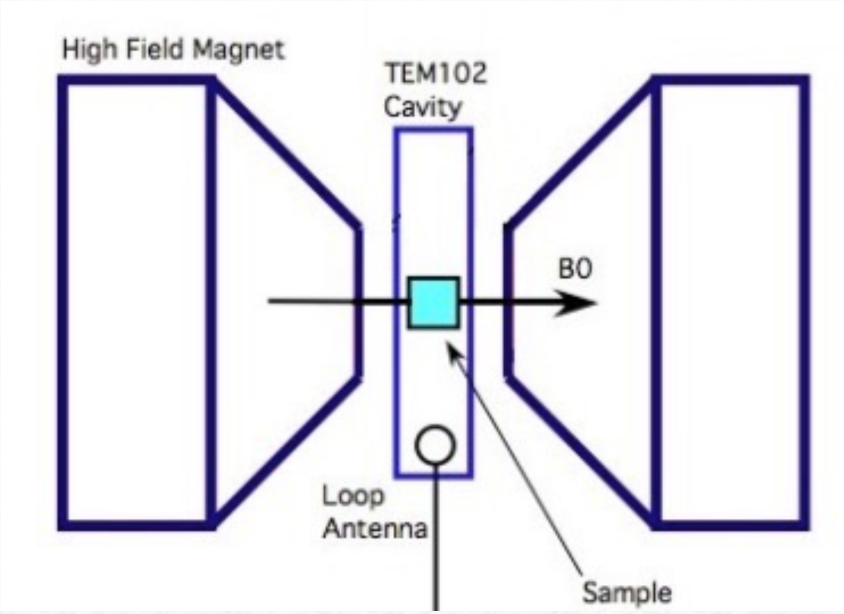

$$B = \begin{pmatrix} B_1 \cos(\omega t) \\ B_1 \sin(\omega t) \\ B_0 \end{pmatrix}$$

$$\nu_L = \mathbf{g}\, \mathbf{B_0}$$

g = 28 GHz / T

1.7 T -> ν_L = 48 GHz

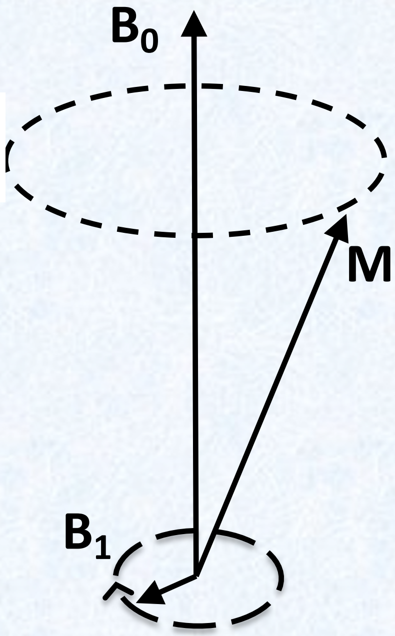

An experimental geometry with **crossed field** is needed:

- **B_0** along the z direction, defines the Larmor resonance
- **RF field B_1** in the x-y plane excites the Magnetization modes

The system macroscopic dynamics is given by **Bloch equations** which describe the evolution of **each component** of the magnetization vector **M.** **No radiation damping in a resonant cavity and in strong coupling regime of Kittel/cavity modes.**

TEM102 Resonant Cavity

B_0 along z axis (normal to the figure)

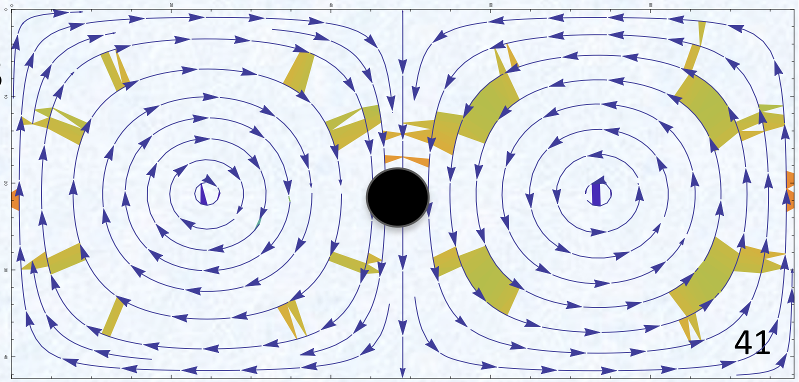

Axion driving of magnetization

The axion wind mimics the transverse rf magnetic field inducing a **time dependent magnetization of the uniform or Kittel mode** of the magnetized sample

$$M_a(t) = \gamma \mu_B B_a n_S \tau_{\min} \cos(\omega_a t),$$

at resonance

τ_{min} **is the shortest coherence time** among:

- **axion wind** coherence $\tau_{\nabla a}$
- magnetic material **relaxation time τ_2**
- **radiation damping τ_r**

n_s – material spin density

μ_B – Bohr magneton

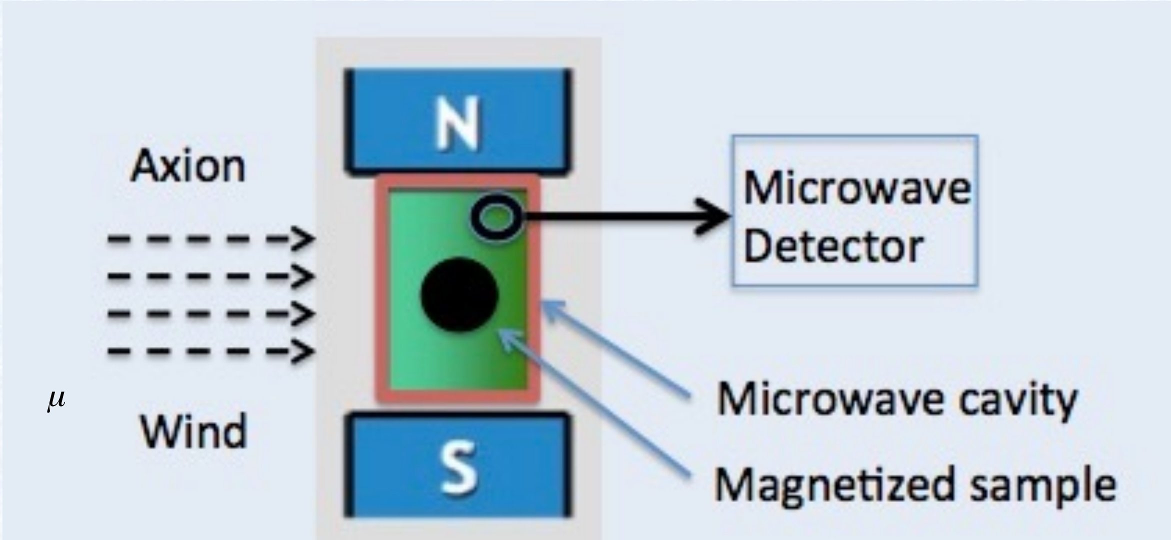

A **volume V_s of magnetized material** will absorb energy from $\mathbf{B}_a$ at a rate

$$P_{\rm in} = \mu_0 \mathbf{H} \cdot \frac{d\mathbf{M}}{dt} = B_a \frac{dM_a}{dt} V_s = \gamma \mu_B n_S \omega_a B_a^2 \tau_{\min} V_s$$

this power will excite magnetization/cavity modes and could be possibly detected

Anticipated signal strength

Expected signal as a function of relevant experimental parameters

Working @ m_a = 200 meV-> 48 GHz

Larmor frequency tuning by magnetizing field
B_0 = 1.7 T => 48 GHz

$$P_{\rm out} = \frac{P_{\rm in}}{2} = \mathbf{3.8 \times 10^{-26}} \left(\frac{m_a}{200\ \mu{\rm eV}}\right)^3 \left(\frac{V_s}{100\ {\rm cm}^3}\right) \left(\frac{n_S}{2\cdot 10^{28}/{\rm m}^3}\right) \left(\frac{\tau_{\rm min}}{2\ \mu{\rm s}}\right)\ {\rm W}$$

Such a low power level is out of reach of linear amplifiers → **Single photon microwave detection**

To be developed

See discussion in *S.K. Lamoreaux et al., Phys. Rev. D 88 (2013) 035020.*

The corresponding **signal photon rate**

$$R_a = \frac{P_{\rm out}}{\hbar\omega_a} = \mathbf{1.2 \times 10^{-3}}\ {\rm Hz}$$

this rate establishes the required dark count rate of the photon counter

Frequency tuning

In order to **scan different mass values**, a frequency tuning of the system must be present

With the QUAX apparatus this can be easily achieved by changing the magnetizing field.

The minimum separation of the peaks is

$$g_m = \gamma \sqrt{\mu_0 \hbar \omega_m n_S V_S / V_c}$$

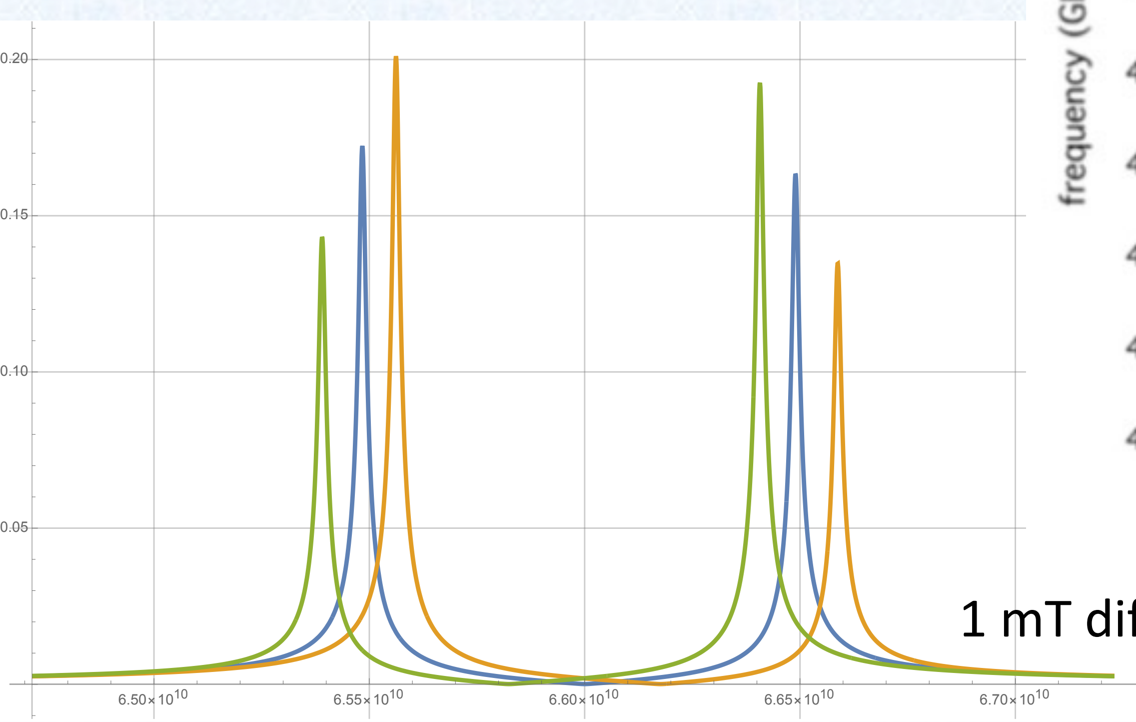

1 mT difference

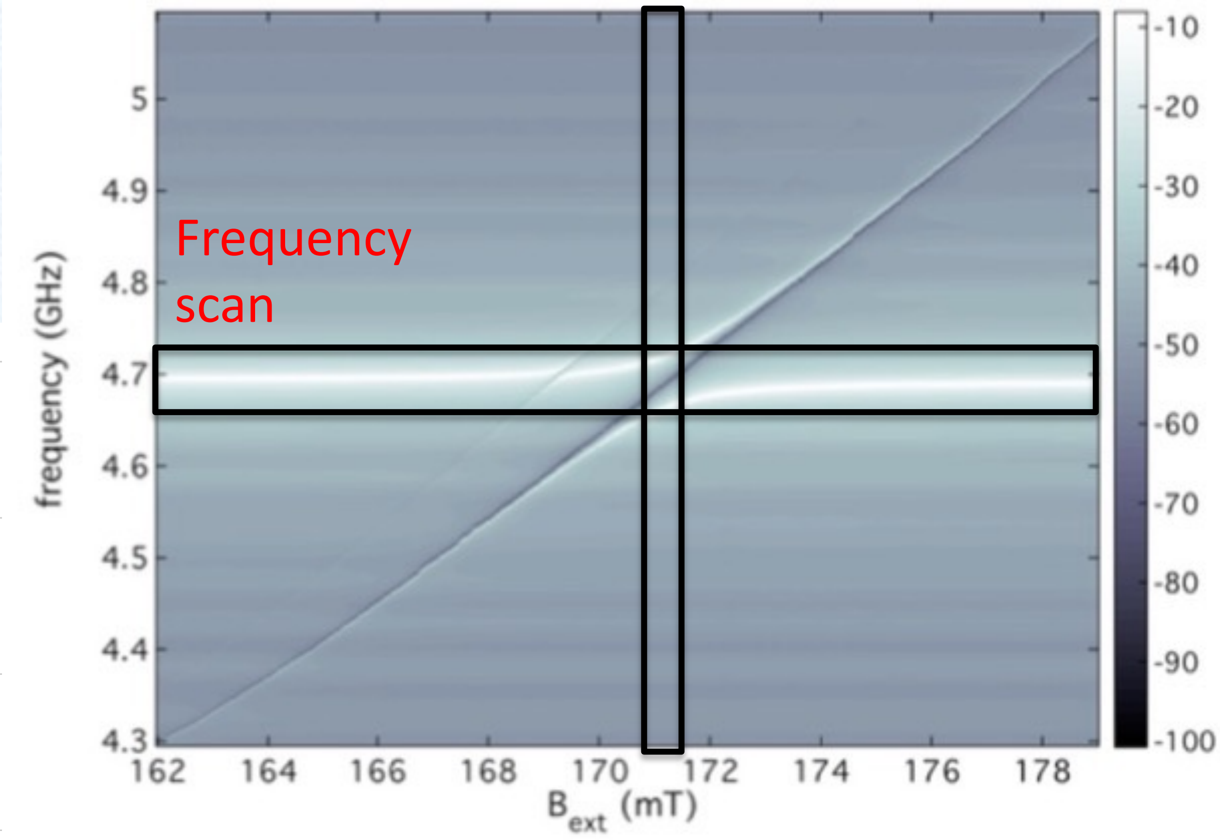

Check coupling with material

Static Magnetic field: homogeneity

A **uniform magnetic field** is important in many different experimental situations.

The degree of required uniformity depends on the kind of experiment. It can be as good as **0.1 ppm for high resolution NMR spectroscopy**.

In our experiment we need an homongeneity at the **ppm level** to **avoid inhomogeneous line broadening** of the Larmor resonance **over the sample volume**.

The simplest strategy to obtain an uniform field is the superimposition of the magnetic field generated by **three coils**: two of them act as an **Helmholtz coil** system and one as **a main field generator**.

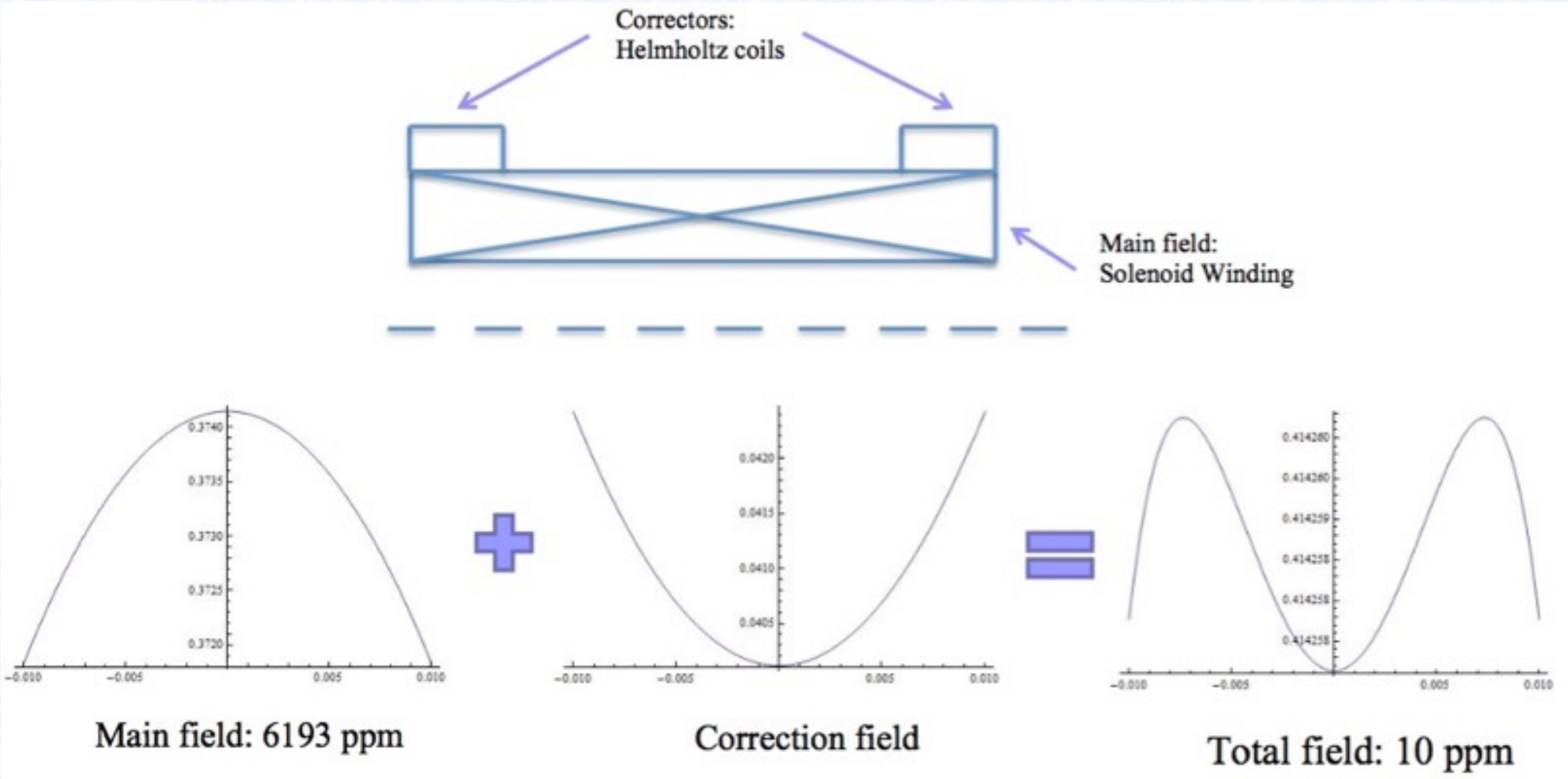

Courtesy U. Gambardella

Magnetic material

Material	Spin density	M0	t_1	t_2	Size
YIG	2.1 x 10^{28} [1/m^3]	1.4 10^5 A/m	0.3 μs	0.3 μs	1 mm, 2 mm and 3 mm diam.

YIG – Yttrium Iron Garnet is a ferrimagnetic synthetic garnet with chemical composition $Y_3Fe_5O_{12}$.
Its **ferrimagnetic linewidth** (= 1 / 2 p t_2) depends on temperature, **sample purity** and geometry (higly polished spheres)

Procurement very difficult → In house development

1. Get high-purity YIG monocrystal from vendors
2. Cut in small cubes roughly 3 mm side
3. First grinding with diamond grinder to get spheres of about 2mm diameter
4. Eight steps of grinding with SiC sand paper down to 3 μm grit size
5. Polishing with 0.5 alumina powder
6. Annealing of the spheres in Oxygen atmosphere

Magnetic material II

Linewidth of sphere at different working stages

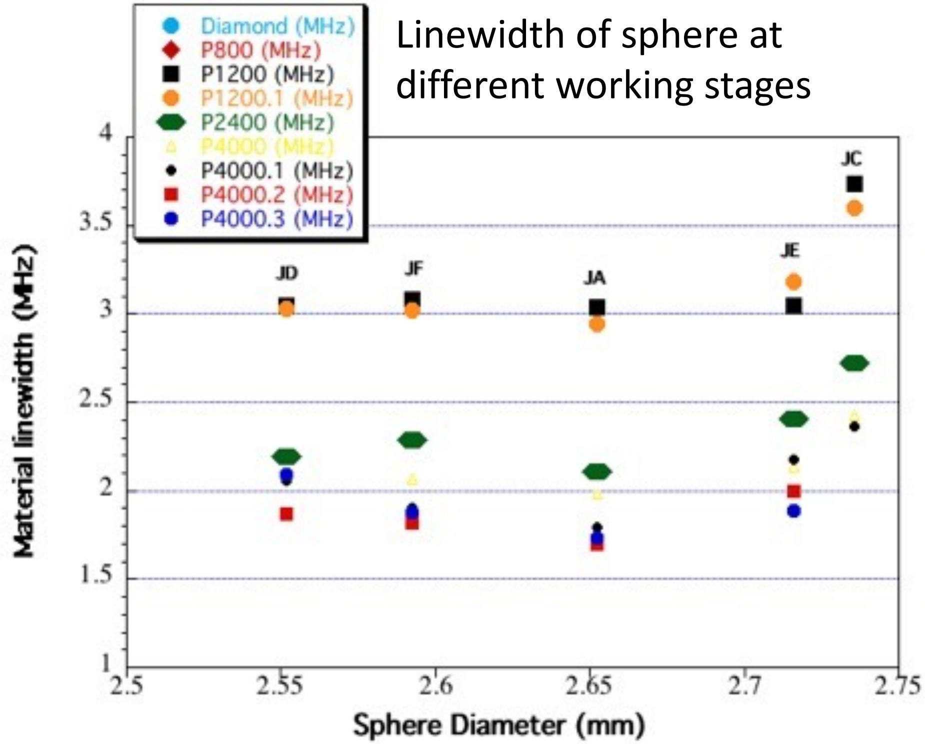

- Homemade production of spheres resulted in 10 spheres with similar diameter (within a few %)
- This allowed to mount the 10 spheres in the same cavity and have strong coupling between all of them and the cavity mode

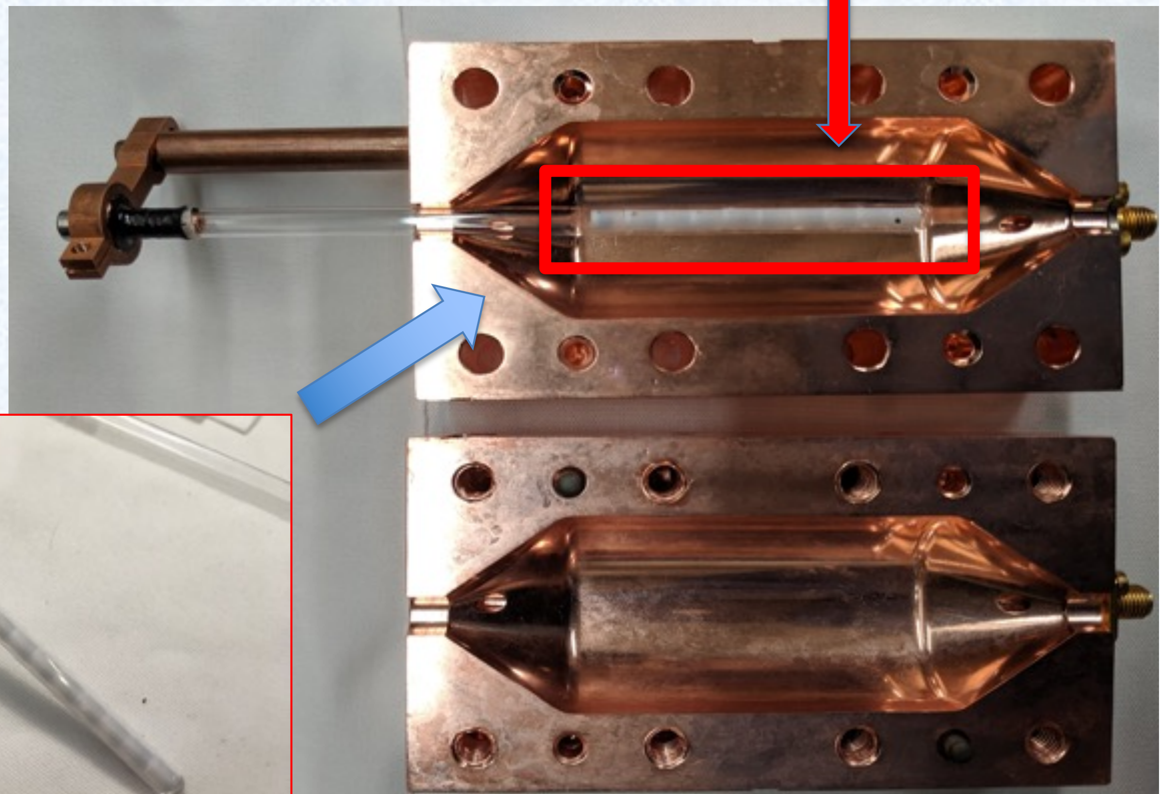

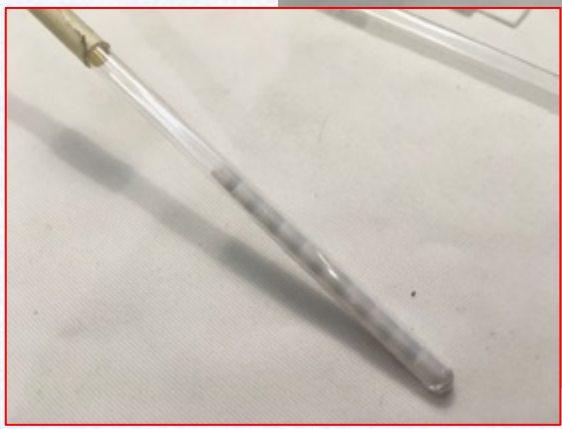

10 spheres-cavity coupling plot